We acknowledge the contribution and collaboration of:

Crotone Province (KR)
www.provincia.crotone.it

The Marine Protected Area “Capo Rizzuto”
www.riservamarinacaporizzuto.it

The International Association of Sedimentologists
www.sedimentologists.org

Under the patronage of:

The Italian Paleontological Society

The Italian Geological Society

The International Fossil Coral Reef society

IFAA - Le Castella - Capo Colonna - Belcastro - Field Trip

Valentina A. Bracchi[a,b], Pietro Bazzicalupo[a], Edoardo Perri[c], Mario Borrelli[c] and Daniela Basso[a,b]

[a]*Dipartimento di Scienze dell'Ambiente e della Terra, Università degli studi di Milano-Bicocca, Piazza della Scienza 4, 20126 Milano, Italy;*
[b]*CoNISMa, Piazzale Flaminio 9, 00196 Roma, Italy*
[c]*Dipartimento di Biologia, Ecologia e Scienze della Terra, Università della Calabria, via Pietro Bucci, 87036 Arcavacata di Rende, Cosenza, Italy*

Contents

1. ITALY

The geological history of the Italian peninsula is fascinating, but also extremely complex.
The oldest rocks in Italy include oceanic crust subducted during the Caledonian orogeny and 440 million year old Ordovician granites. Overall, Italian Paleozoic rocks commonly show evidence of the Hercynian orogeny in the Alps, Sardinia, the Apuan Alps in Tuscany, and the Peloritani mountains of Sicily and Calabria.
During Mesozoic, the opening of the west branch of the Tethys Ocean reoriented sections of Italy atop the Adriatic Plate (Africa domain) and created the Ligure-Piemontese oceanic basin, leading to widespread deposition of carbonates and evaporites. During this time, the oceanic basin continued to deepen, following the divergent movement of the Northern Eurasia and Southern African (including the Adriatic) plate.
Starting from the Paleocene, because of the opening of the Southern Atlantic ocean, the change in interaction between Eurasia and Africa accompanied the closure of the Ligure-Piemontese ocean basin and resulted in tectonic compression along the Adriatic Plate's northern margin, kicking off the formation of the Alps and the Apennines.
The consumption and subduction of the Ligure-Piemontese ocean basin, together with the subsequent crustal collision and uplift are all phenomena that contribute to the inception and development of the Alpine chain, as we know it today. The Alps represent the most iconic Italian mountain chain, representing the natural boundary of the Northern Italian territory, in its famous shape as an arch.
The Apennine orogeny started In the Eocene. It evolved independently from the Alps as the result of a new west-dipping subduction and continental collision between Corsica-Sardinia block, counter-clock rotated from the south of France, and Adria microplate. As the Adria microplate migrated to the northeast with an anti-clockwise rotation, Apennine foredeeps migrated to the east assuming their NW-SE alignment, designing the Italian outline.
During the Miocene, the ongoing uplift affected Alps as well as the Paleo-Apenninic chain and backarc to foredeep basins continued developing. The opening of backarc basins like the Tyrrhenian Sea caused the Calabro-Peloritano block to be separated from Sardinia, moving further south-east and finally included in the southern apennines arc, exactly in correspondence with the Calabria region. Since the Pleistocene, uplift, in both chains, continues.

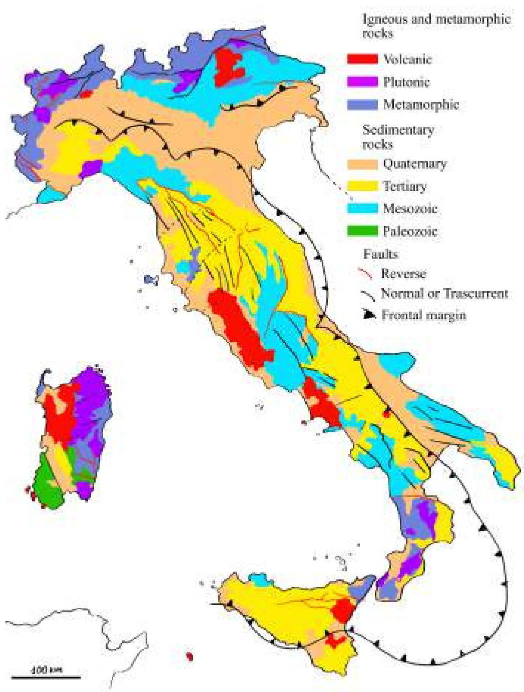

Figure 1. The simplified structural map of Italy, modified from Bosellini, 2017.

2. CROTONE BASIN: GEOLOGICAL AND STRATIGRAPHIC SETTING

The Calabrian Arc is an arcuate terrane connecting the Southern Apennine (NW-trending) chain with the Sicilian Maghrebides (E-trending), separating the Ionian and Tyrrhenian basins. Because of the roll-back of a NW-dipping subduction of the Ionian oceanic slab, the Calabrian Arc migrated south-eastward from mid-Miocene onwards [1-6] with fragmentation and formation of intra- and fore-arc sedimentary basins on both Tyrrhenian and

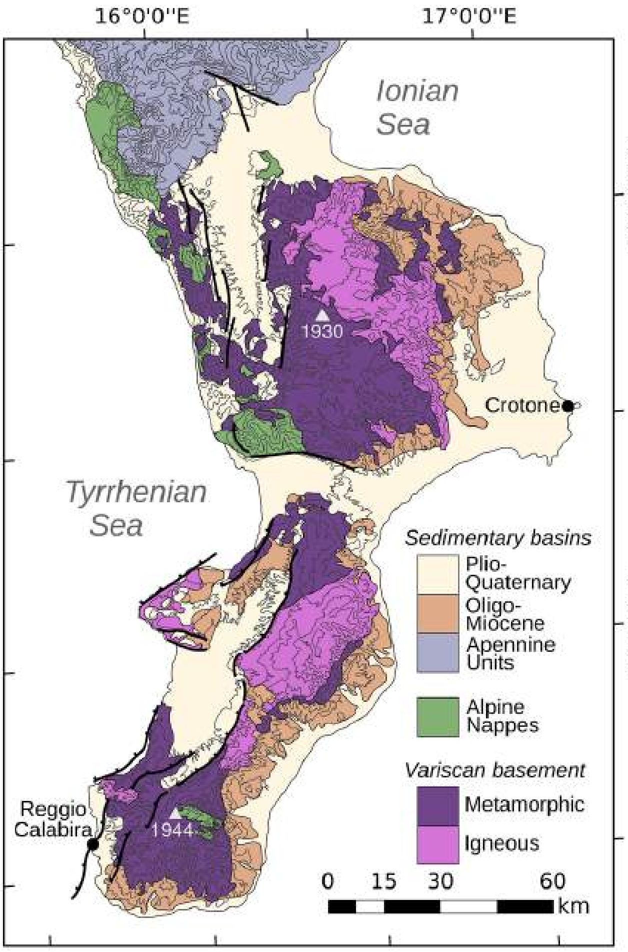

Figure 2. Simplified geological map of Calabria (from Quye-Sawyer et al., 2021)

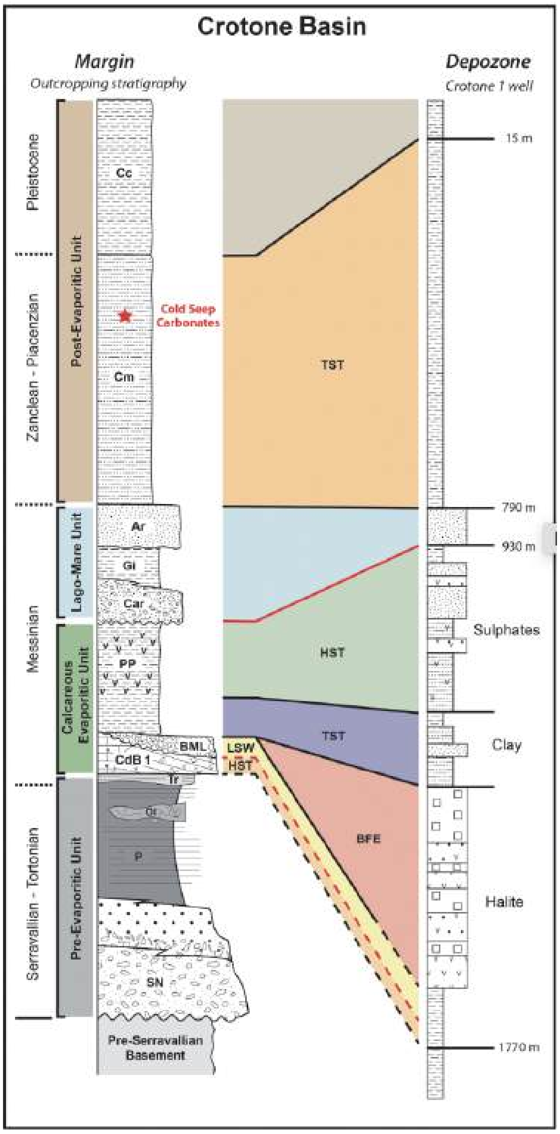

Figure 3. General Serravallian–Pleistocene stratigraphy of the Crotone Basin. The outcropping stratigraphy is not to scale. SN: San Nicola Formation, P: Ponda Formation, Tr: Tripoli Formation, CdB: Calcare di Base Formation, BML: Breccia Madama Lucrezia, PP: Petilia Policastro Formation, Car: Carvane Conglomerates Formation, Gi: Gigli Formation, Ar: Arvano Formation, Cm: Cavalieri Marls, Cc: Cutro Clay, Ol: Olistostrome. TST: transgressive systems tract; HST: highstand systems tract; LSW: lowstand wedge; BFE: basin-fill evaporites (from Perri et al., 2024)

Ionian sides of Calabria, which in turn controlled the development of the basin sedimentary infills [e.g. 9-11].

The Crotone basin is one of those sedimentary infills. It is a segment of the Ionian fore-arc basin located on the internal part of the Calabrian accretionary wedge [12-14]. Its development started between the Serravallian and the Tortonian age [1, 6, 15-19]. The architecture of its sedimentary infill recorded complex regional-scale tectonic events, which led to alternating phases of subsidence and uplift [20-21].

The basin bedrock consists of crystalline Paleozoic rocks [19, 22, 23], with an accumulation of continental and shallow-to deep- marine deposits on top, following the Tyrrhenian Sea opening [24-26]. The sedimentary infill started with a transgressive Pre-Evaporitic Unit (Serravallian–Lower Messinian), that shows a maximum thickness of 300 m. It includes conglomerates and sandstones of the San Nicola Formation, which grade upward into deep marine Tortonian to early Messinian clays of the Ponda Formation. At the top, it is covered by the Tripoli Formation, which includes finely laminated diatomites [22, 27, 28].

The Messinian represents a pivotal moment for the Mediterranean Region [29]. The so-called salinity crisis affected the Mediterranean Sea, during which a large portion of the Sea dried. This translates in the deposition of thick evaporites, including two depositional members named 'Calcareous-Evaporitic' (CE) and 'Lago-Mare' Units [27, 28, 30].

The CE Unit begins with the Calcare di Base Formation, 60 m in thickness, constituted by carbonate and evaporite facies, and corresponding to a highstand phase [27].

Above it, a clastic body occurs, up to 50 m in thickness, characterized by coarse to very coarse debrites with gypsum, carbonate and terrigenous clasts, together with minor primary autochthonous shallow-water evaporites. This suggests a sea-level fall, and this interval is ascribed to a lowstand wedge that predates the development of a massive basinal evaporitic body (halite dominated) occurring during the late lowstand phases as basin-fill evaporites. The Messinian halite occurs in the whole subsurface of the Crotone Basin and has a variable thickness ranging between 150 and 200 m, controlled by the basin architecture. The top of the CE Unit shows grayish clays and clayey marls, including meter-scale laminated and nodular gypsum, interpreted as a renewed transgressive and highstand phase. The Lago-Mare Unit follows in the succession and possibly indicates a post-evaporitic freshwater input from the Paratethys [31]. This Unit is widespread in the Crotone Basin and is characterized by a thick alluvial conglomeratic body (Carvane Conglomerates Formation) at the base, overlain by clays (Gigli Formation) and sandstones (Arvano Formation) [21, 22]. After the Messinian Salinity Crisis, the reflooding of the Mediterranean marks the beginning of the Pliocene, with a transgressive Post-Evaporitic Unit corresponding to a thick clayey to marly formation

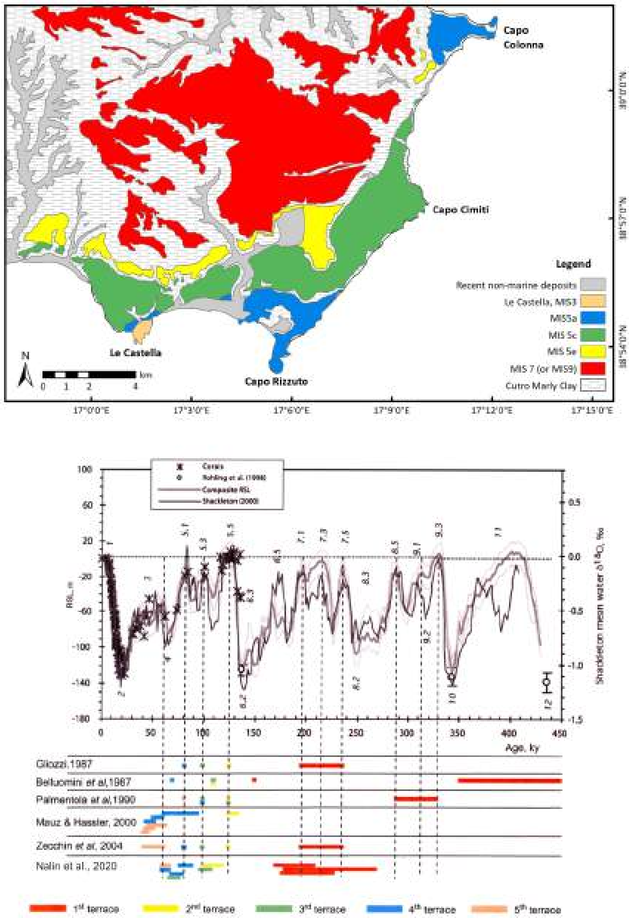

Figure 4. Simplified map of the Crotone peninsula with the indication of the five marine terraces, and the relative chronostratigraphic interpretations (modified from Nalin, 2006).

(Cavalieri Marls Formation), reaching a thickness of up to 1000 m. It is composed of shelf to slope claystones and siltstones intercalated with centimeter to decimetre-thick turbidite layers, [19-21]. Upward, it is overlain by similar claystones, Piacenzian to mid Pleistocene in age, named the Cutro Clay Formation, which has a maximum thickness of ca 500 m. Cutro Clay Fm locally includes turbidite beds, sapropels, diatomites and ash beds.

From the mid-Pleistocene, this region has been affected by significant uplift [32, 33], which, in combination with glacio-eustatic sea level oscillations, results in the development of flights of marine terraces, especially along the Ionian coasts of the Calabria region [34-37]. In the Crotone peninsula, Zecchin et al. [38] distinguished five orders of terraces that unconformably overlay the Cutro Marly Clay Formation (Figure 4), with the different chronostratigraphic interpretations modified from [39].

Despite this general uplift context, there is an important subsidence process involving the Crotone Basin and in particular the Crotone Peninsula until today, which is related to the activity of the so-called Crotone megalandslide [23, 40]. The slide includes both an onshore updip extensional domain, possibly connected with a curved seaward-dipping fault system to the NW, and an offshore downdip compressional domain through a buried detachment surface lying at a Messinian halite layer [41]. The slide involves a landmass including the Messinian-Pleistocene deposits since Zanclean, and after a phase of inactivity during the Calabrian, it underwent a second reactivation since middle Pleistocene due to regional uplift, which seems to involve especially the Crotone peninsula[40].

2.1. References

1. Malinverno, A., Ryan, W.B.F. (1986). Extension in the Tyrrhenian Sea and shortening in the Apennines as a result of arc migration driven by sinking of the lithosphere. *Tectonics*, 5, 227–245.
2. Patacca, E., Sartori, R., Scandone, P. (1990). Tyrrhenian basin and Apenninic arcs: kinematic relations since late Tortonian times. *Memor. Soc. Geol. Ital.*, 45, 425-451.
3. Sartori, R. (1990). The main results of ODP Leg 107 in the frame of Neogene to Recent geology of peri-Tyrrhenian areas. *Proceedings of the Ocean Drilling Program, Scientific Results*, 107, 715-730.
4. Gueguen, E., Doglioni, C., Fernandez, M. (1998). On the post-25 Ma geodynamic evolution of the western Mediterranean. *Tectonoph.*, 298 (1–3), 259-269.
5. Faccenna, C., Becker, T.W., Lucente, F.P., Jolivet, L., Rossetti, F. (2001). History of subduction and back-arc extension in the Central Mediterranean. *Geophys. J. Int.*, 145 (3), 809–820.
6. Faccenna, C., Piromallo, C., Crespo-Blanc, A., Jolivet, L., Rossetti, F. (2004). Lateral slab deformation and the origin of the western Mediterranean arcs. *Tectonics*, 23, TC1012.
7. Finetti, I.R., Lentini, F., Carbone, S., Del Ben, A., Di Stefano, A., Forlin, E., Guarnieri, P., Pipan, M., Prizzon, A. (2005). Geological outline of Sicily and lithospheric tectonodynamics of its Tyrrhenian margin from new CROP seismic data. In: R. Finetti (Ed.), *Deep Seismic Exploration of the Central Mediterranean and Italy*, Elsevier, Amsterdam, The Netherlands, pp. 319–375.
8. Del Ben, A., Barnaba, C., Taboga, A. (2008). Strike-slip systems as the main tectonic features in the Plio-Quaternary kinematics of the Calabrian Arc. *Mar. Geophys. Res.*, 29, 1–12.
9. Critelli, S., Muto, F., Perri, F., Tripodi, V. (2017). Interpreting provenance relations from sandstone detrital modes, southern Italy foreland region: stratigraphic record of the Miocene tectonic evolution. *Mar. Petrol. Geol.*, 87, 47–59.
10. Critelli, S. (2018). Provenance of mesozoic to Cenozoic Circum-Mediterranean sandstones in relation to tectonic setting. *Earth Sci. Rev.*, 185, 624–648.
11. Borrelli, M., Perri, E., Morsilli, M., Critelli, S. (2023). Late Permian-Triassic sedimentary evolution of the Southern Adriatic area based on wells and cores analysis. *Mar. Petrol. Geol.*, 150, 106154.
12. Cavazza, W., Blenkinsop, J., De Celles, P.G., Patterson, R.T., Reinhardt, E.G. (1997). Stratigrafia e sedimentologia della sequenza sedimentaria oligocenica–quaternaria del bacino Calabro–Ionico. *Boll. Soc. Geol. Ital.*, 116, 51–77.
13. Bonardi, G., Cavazza, W., Perrone, V., Rossi, S. (2001). Calabria-Peloritani terrane and northern Ionian Sea. In: I.P. Martini, G.B. Vai (Eds.), *Anatomy of an Orogen: The Apennines and Adjacent Mediterranean Basins*, Kluwer Academic Publishers, pp. 287–306.
14. Minelli, L., Faccenna, C. (2010). Evolution of the Calabrian accretionary wedge (Central Mediterranean). *Tectonics*, 29, TC4004.
15. Milia, A., Torrente, M.M. (2014). Early-stage rifting of the southern Tyrrhenian region: the Calabria-Sardinia breakup. *J. Geodyn.*, 81, 17–29.
16. Van Dijk, J., Okkes, M. (1991). Neogene tectonostratigraphy and kinematics of Calabrian basins; implications for the geodynamics of the Central Mediterranean. *Tectonoph.*, 196 (1–2), 23-60.
17. Patacca, E., Scandone, P. (2007). Geology of the southern Apennines. *Boll. Soc. Geol. Ital.*, 7, 75–119.
18. Perri, E., Borrelli, M., Bernasconi, M.P., Gindre-Chanu, L., Spadafora, A., Critelli, S. (2019). Microbial-dominated car-

bonate depositional systems: a biosedimentary and stratigraphic reconstruction in the Late Triassic of Western Tethys (northern Calabria, Italy). *Facies*, 65, 31.

19. Zecchin, M., Civile, D., Caffau, M., Critelli, S., Muto, F., Mangano, G., Ceramicola, S. (2020). Sedimentary evolution of the Neogene-Quaternary Crotone Basin (Southern Italy) and relationships with large-scale tectonics: a sequence stratigraphic approach. *Mar. Petrol. Geol.*, 117, 104381.
20. Zecchin, M., Caffau, M., Civile, D., Critelli, S., Di Stefano, A., Maniscalco, R., Muto, F., Sturiale, G., Roda, C. (2012). The Plio-Pleistocene evolution of the Crotone Basin (southern Italy): interplay between sedimentation, tectonics and eustasy in the frame of Calabrian Arc migration. *Earth Sci. Rev.*, 115, 273–303.
21. Massari, F., Prosser, G. (2013). Late Cenozoic tectono-stratigraphic sequences of the Crotone basin; insights on the geodynamic history of the Calabrian Arc and Tyrrhenian sea. *Basin Res.*, 25, 26–51.
22. Massari, F., Prosser, G., Capraro, L., Fornaciari, E., Consolaro, C. (2010). A revision of the stratigraphy and geology of the south-western part of the Crotone Basin (South Italy). *Ital. J. Geosci.*, 129, 353–384.
23. Zecchin, M., Accaino, F., Ceramicola, S., Civile, D., Critelli, S., Da Lio, C., Mangano, G., Prosser, G., Teatini, P., Tosi, L. (2018). The Crotone Megaland slide, southern Italy: architecture, timing and tectonic control. *Sci. Rep.*, 8, 7778.
24. Vai, G.B., Martini, J.P. (2001). Anatomy of an Orogen: The Apennines and the Adjacent Mediterranean Basins. Kluwer Acad., Norwell, MA, pp. 287–306.
25. Mattei, M., Cipollari, P., Cosentino, D., Argentieri, A., Rossetti, F., Speranza, F., Di Bella, L. (2002). The Miocene tectono-sedimentary evolution of the southern Tyrrhenian Sea: stratigraphy, structural and palaeomagnetic data from the on-shore Amantea basin (Calabrian Arc, Italy). *Basin Res.*, 14, 147-168.
26. Cavazza, W., Ingersoll, V.R. (2005). Detrital modes of the Ionian forearc basin fill (Oligocene Quaternary) reflect the tectonic evolution of the Calabria - Peloritani terrane (Southern Italy). *J. Sediment. Res.*, 75, 268-279.
27. Borrelli, M., Perri, E., Critelli, S., Gindre-Chanu, L. (2021). The onset of the Messinian Salinity Crisis in the central Mediterranean recorded by pre-salt carbonate/evaporite deposition. *Sedimentology*, 68, 1159–1197.
28. Borrelli, M., Perri, E., Avagliano, D., Coraggio, F., Critelli, S. (2022). Paleogeographic and sedimentary evolution of North Calabrian basins during the Messinian Salinity Crisis (South Italy). *Mar. Petrol. Geol.*, 141, 105726.
29. Gautier, F., Clauzon, G., Suc, J.P., Cravatte, J., Violanti, D. (1994). Age and duration of the Messinian salinity crisis. *C.R. Acad. Sci., Paris (IIA)*, 318, 1103–1109.
30. Gindre-Chanu, L., Borrelli, M., Caruso, A., Critelli, S., Perri, E. (2020). Carbonate/evaporitic sedimentation during the Messinian salinity crisis in active accretionary wedge basins of the northern Calabria, southern Italy. *Mar. Petrol. Geol.*, 112, 104066.
31. Roda, C. (1964). Distribuzione e facies dei sedimenti neogenici nel Bacino Crotonese. *Geol. Romana*, 3, 319–366.
32. Westaway, R. (1993). Quaternary uplift of Southern Italy. *J. Geophys. Res.*, 98 (B12), 21741–21772.
33. Westaway, R., Bridgland, D. (2007). Late Cenozoic uplift of Southern Italy deduced from fluvial and marine sediments: coupling between surface processes and lower-crustal flow. *Quat. Int.*, 175, 86–124.
34. Gliozzi, E. (1987). I terrazzi marini del Pleistocene superiore della penisola di Crotone (Calabria). *Geol. Romana*, 26, 17–79.
35. Palmentola, G., Carobene, L., Mastronuzzi, G., Sansò, P. (1990). I terrazzi marini pleistocenici della Penisola di Crotone (Italia). *Geogr. Fis. Din. Quat.*, 13, 75–80.
36. Cucci, L., Cinti, F.R. (1998). Regional uplift and local tectonic deformation recorded by the Quaternary marine terraces on the Ionian coast of Northern Calabria (southern Italy). *Tectonophysics*, 292, 67–83.
37. Santoro, E., Mazzella, M.E., Rerranti, L., Randisi, A., Napolitano, E., Rittner, S., Radtke, U. (2009). Raised coastal terraces along the Ionian Sea coast of Northern Calabria, Italy, suggest space and time variability of tectonic uplift rates. *Quat. Int.*, 206, 78–101.
38. Zecchin, M., Nalin, R., Roda, C. (2004). Raised Pleistocene marine terraces of the Crotone peninsula (Calabria, southern Italy): facies analysis and organization of their deposits. *Sediment. Geol.*, 172, 165–185.
39. Nalin, R. (2006). Marine terraces of the Crotone Peninsula (Calabria) and insights into red-algal deposits from central Mediterranean and New Zealand. PhD thesis, XVIII cycle, Università degli studi di Padova, Dipartimento di Geologia, Paleontologia e Geofisica.
40. Minelli, L. et al. (2013). Discovery of a gliding salt-detached megaslide, Calabria, Ionian Sea, Italy. *Geophys. Res. Lett.*, 40, 4220–4224.
41. Mangano, G., Zecchin, M., Civile, D. (2020). Large-scale gravity-driven phenomena in the Crotone Basin, southern Italy. *Mar. Petrol. Geol.*, 117.
42. Bosellini, A. (2017). Outline of the geology of Italy. *Landscapes and landforms of Italy*, 21-27.
43. Quye-Sawyer, J., Whittaker, A. C., Roberts, G. G., Rood, D. H. (2021). Fault throw and regional uplift histories from drainage analysis: Evolution of southern Italy. *Tectonics*, 40(4).

3. HISTORICAL BACKGROUND ON LE CASTELLA AND CAPO COLONNA

Le Castella, a small village placed in the SW sector, and Capo Colonna, an archaeological site toward SE, are the two localities that outline the geographical extension of the Crotone Peninsula. The human presence of the peninsula dates back to the Bronze Age, and several important historical episodes, among which some of the myths like Argonauts of Ulisses passage, are reported in literature.

Capo Colonna is a geographic toponymy to indicate the promontory, and it hosts the last column of the *Hera Lacinia* doric temple, built around 480-470 BC. The site has been sacred since the IV century BC. Here was the *Heraion*, the sacred site in honor of the god *Hera Lacinia*, used by the citizens of the Achaean colony of *Kroton* (= actual Crotone).

Le Castella was the subject of many legends and even the island of Calypso described by Homer in his Odyssey should be located right in the vicinity of the village. The primitive form of today's name is given, following the departure of Hannibal after the Second Punic War, from the settlement of 3000 Roman colonists who gave the place its name as *Castra*. There are hypotheses that before the Roman settlement there was another founded by Hannibal, of which Pliny mentions it as *Castra Annibale*. The actual name includes the plural designation with the article *"Le"* and *"Castella"* in Latin. The origin of *"Le"* is not yet clear: it could be due to a legend according to which many fortifications or homes built on a disappeared archipelago and on the mainland. For sure, it is not related to the wonderful Aragonese castle which instead represents the present-day icon of the village. The current fortress rests on foundations dating back to the Magno-Greek period (400 BC).

4. CORALLIGENOUS AND RHODOLITH BEDS FROM LATE PLEISTOCENE MARINE TERRACES

Exploring the euphotic and mesophotic algal reefs, as well as rhodoliths, from Late Pleistocene marine terrace deposits of Crotone peninsula (Fig. 4) offers a unique opportunity to delve into the geological history and paleoenvironmental conditions of the Crotone Basin. By studying deposits from Marine Isotope Stage 3 in Le Castella and Marine Isotope Stage 5a (or 5.1) in Capo Colonna (Fig. 4), participants will gain insights into how paleoenvironmental and paleogeographic factors influenced the formation of carbonate factories dominated by coralline algae deposits [1, 2].

Coralline algae are autogenic habitat engineers responsible for the formation of intertidal algal rims, subtidal rhodoliths, and algal reefs known in the Mediterranean as *Coralligène* (= Coralligenous). In the Mediterranean Sea, Coralligenous presently forms hard biogenic substrate mainly produced by the superposition of several generations of calcareous red algae living in dim light conditions[3]. Although it has been originally indicated as the ecological climax for the Mediterranean circalittoral zone [4, 5], further studies recognized Coralligenous also in dim-light infralittoral settings [6-13]. Coralligenous develops on both hard and soft bottoms, generating rims on submarine vertical cliffs or caves, and discrete columns up to metrical tabular banks on sub-horizontal soft or hard substrates [14]. Several associations and facies have been described under the term Coralligenous [3, 15-17], as the results of the interplay between biotic and abiotic factors (light exposure, availability of trophic resources, substrate exposure, sedimentation rate, freshwater influence, and biotic interaction) playing a crucial role in shaping the various facies of Coralligenous [e.g. 10, 18-26]. Several species of calcareous red algae Corallinophycidae (crustose coralline algae, CCA) and some calcareous Peyssonneliales are characteristic habitat-engineers [3,4, 5, 23, 26-29] and the volumetrically most important fossil framework builders in Coralligenous [1, 2, 30-33). Other important builders are bryozoans, polychaetes, and cnidarians [3, 17, 34]. Bryozoans producing large, long-lived, habitat-forming colonies can be primary builders [20, 27, 35, 36]. Rhodoliths are unattached nodules of calcareous red algae [37-40] showing large morphological variability between three end-members: unattached branches, praline rhodoliths and boxwork rhodoliths [39-41]. In the Mediterranean bionomic model [4, 5] rhodolith beds may occur as a facies of the Coastal Detritic biocoenosis, one of the most complex, heterogeneous and widely distributed biocoenosis of the Mediterranean shelf. Although their typical distribution is within the circalittoral zone, rhodolith beds are also reported from the Mediterranean infralittoral [42].

5. LE CASTELLA MARINE TERRACE (4 September)

The Upper Pleistocene deposits of Le Castella marine terrace (Calabria, Southern Italy) represent one of the few examples of fossil Mediterranean coralligenous. Here, the genesis and development of shallow coralligenous facies and its spatial heterogeneity can be observed.

Le Castella marine terrace outcrops in the southwestern side of the Crotone peninsula, where it has an extension of less than 1 km2. Its age has been correlated with Marine Isotope Stage 3 (56$\pm$10 ka), on the basis of field stratigraphic considerations [43], luminescence dating [44, 45] (Fig. 4). Preliminary observations of the Le Castella terrace deposits were provided by [43, 46] followed by a more extensive work by [2, 46]. The terrace is gently inclined seaward (SE), with an elevation ranging between ~15 m above sea level at the inner margin, to below sea level at its distal portion. The deposit constitutes an unconformity-bounded, transgressive-regressive cycle. The paleocliff is roughly NE-SW directed, and marked by a gentle morphological step between 15 and 20 m above sea level. The terrace deposits are well exposed along the present-day coastline, varying in thickness from ~3 m in the proximal part of the terrace up to ~10 m seaward.

5.1. Sequence stratigraphy

Le Castella marine terrace deposits preserved different facies related to different phases of the MIS3 during transgressive–regressive cycle.

A transgressive trend can be inferred between the basal conglomerate, interpreted to have formed by seacliff retreat and wave erosion at intertidal to subtidal depths (Fig. 5A), to the overlying fully subtidal coralligenous (Fig. 5B). Coralligenous developed in relative shallow-waters and the adjacent biocalcarenite included infralittoral setting dead assemblages, thus suggesting the occurrence of a mosaic of infralittoral paleohabitats, including meadows. In the outer portion of Le Castella deposits, a normal fault together with the formation of a sedimentary spit, partially inhibits the development of Coralligenous (Fig. 5C). The deposits above the Coralligenous includes biocalcarenite, and show a regressive progradational trend (Fig. 5D). Although the coralligenous build-ups are bracketed between transgressive and regressive deposits, the exact positioning of the maximum flooding is still uncertain, although constrained in infralittoral settings.

5.2. Coralligenous

Le Castella marine terrace preserves a remarkable example of large-sized coralligenous build-ups (up to 3 m) that developed in a shallow-water (<20 m of water depth), possibly infralittoral, setting (Fig. 6). The build-ups and associated biocalcarenites (Fig. 7) document a complex spatial paleo seascape mosaic, with Coralligenous hybrid banks (Stop 1) laterally adjacent to shallow water mobile sediments rich in bioclasts, derived from both infralittoral and circalittoral assemblages. The biocalcarenite preserves spectacular sedimentary structures (Fig. 8), such as trough-cross bedding in the lower portion and planar lamination

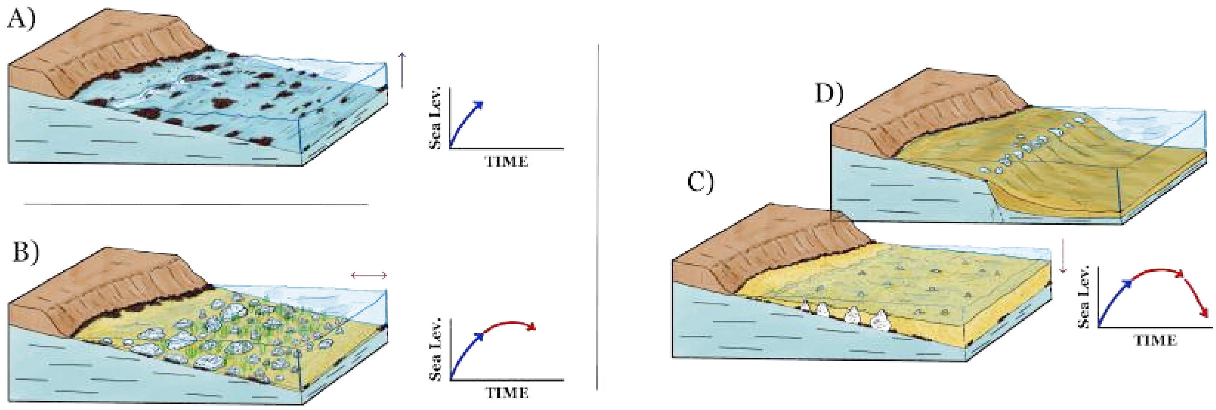

Figure 5. Interpretative scheme of the Le Castella marine terrace. A) The transgressive phase with the development of the basal conglomerate by seacliff retreat and wave erosion at intertidal to subtidal depths; B) the highstand phase with the development of a mosaic of infralittoral habitats, including shallow Coralligenous and possibly meadows; C) the regressive phase with the deposition of bioclastic sediment burning the Coralligenous build-ups; D) the outer sector of Le Castella marine terrace deposits showing the occurrence of a sedimentary spit and a normal fault that inhibits the development of coralligenous.

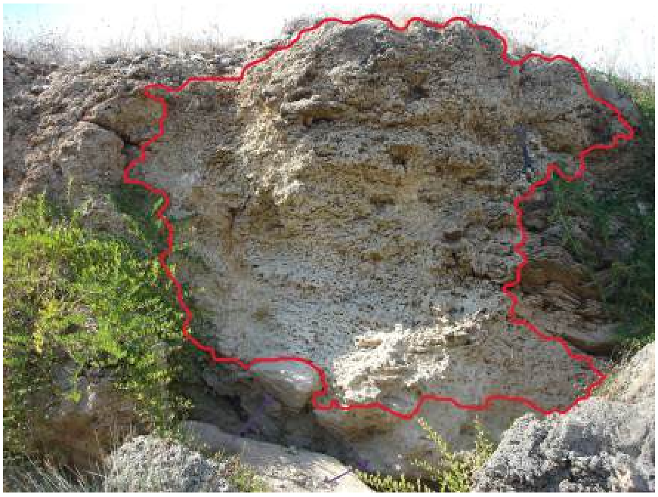

Figure 6. The inner, northern Coralligenous hybrid banks (red contour) of Le Castella. Hammer as scale. Note the basal conglomerate blocks (purple arrows).

in the uppermost part (Stop 2).
In most cases, the inception of Coralligenous in Le Castella occurs over stable cobbles and boulders (= basal conglomerate) collapsed from older terrace deposits during sea cliff retreat under transgressive phase (Stop 1 and 3) (Fig. 6, arrows). The non-uniform cover on the basal ravinement surface is due to the absence of large stable clasts on a shallow-water mobile bottom preventing the coralligenous development, and resulting in inter-banks areas characterized by biogenic sediments (Stop 2). Heterogeneity in size, structure of the algal framework, and composition of coralligenous facies over short distances of a few hundred meters have been reconstructed from inner, norther, to distal, southern portion of the terrace in Le Castella (Stop 1 versus Stop 4), possibly due to variations in sedimentation rate and water turbidity. In particular, the abundance of fine-grained sediment associated with the Coralligenous of the southern sector (Stop 4) of Le Castella suggests higher levels of settling of suspended load than in the northern banks (Stop 1).

Figure 7. The coarse biocalcarenite that is laterally adjacent to Coralligenous build-ups.

Figure 8. The sedimentary structures of the biogenic calcarenite, showing evident trough cross-bedding alternated with layers with no sedimentary structures. Hammer as scale.

The inner, northern Coralligenous (Stop 1) consists of hybrid

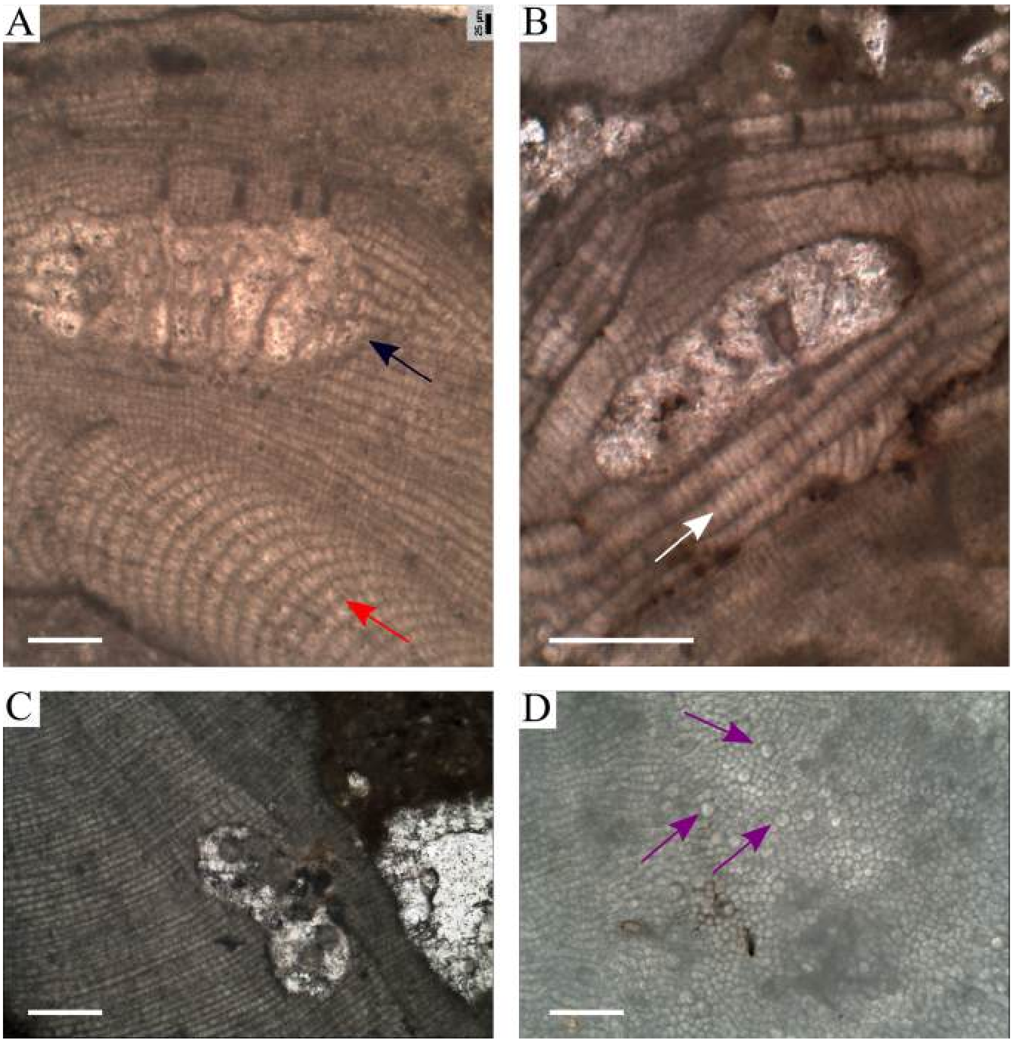

Figure 9. Crustose coralline algae identified in the Le Castella marine terrace deposits: A) *Mesophyllum philippii*: tetrasporangial conceptacle (black arrow) and the coaxial hypothallus (red arrow); B) *Titanoderma pustulatum*: tetrasporangial conceptacle and the palisade cells (white arrow); C) *Lithophyllum* gr. *stictiforme*: tetrasporangial conceptacle; D) *Neogoniolithon* sp.: detail of trichocytes (purple arrows). Scale bar is 100 µm.

banks, 1–3 m thick and 3–10 m wide, mushroom–shaped to more tabular, the latter having a rather continuous base and discontinuous upward growing portions (Fig. 6). The Coralligenous framework is dense, crustose, dominated by coralline algae, formed by compacted leafy crusts with a layered/foliose fabric. The most abundant species are *Mesophyllum* spp and *Titanoderma pustulatum*, more rare are *Lithophyllum* gr. *stictaeforme, Neogoniolithon sp.* and *Phymatolithon calcareum* (Fig. 9). In some cases, intensive bioturbation produces a vacuolar aspect. Larger cavities are filled with bioclastic packstone to grainstone, locally displaying festooned stratification, and smaller scale cross-stratification. The build-ups are overlain by a skeletal packstone to grainstone. The grainstone shows an erosional base and has a total thickness variable between 0.5 to 1 m. Locally, the top of the build-ups coincides with the modern topographic surface. The contact between the build-ups and the bioclastic packstone/grainstone at the top is sharp and locally planar, but evidence of erosional truncation is minor in comparison with most of the sites, where the original irregular surface of the build-ups is preserved.

The outer, southern Coralligenous (Stop 4) consists of smaller 1–1.8 m thick build-ups (Fig. 5A-B, 10). Coralligenous apparently shows a lateral continuity of more than 10 m and its overall morphology is tabular at the outcrop scale. It consists of laterally coalesced individual build-ups with an irregular surface. The build-ups show an open framework made of leafy algal crusts filled by a gray silty to sandy matrix. The upper part of the build-ups shows intensive bioturbation. Skeletal remains of bryozoans, mollusks and echinoids are also common. One distinctive aspect of the southern bank is the frequent occurrence of the coral *Cladocora caespitosa* (Stop 3), which in places represents the primary framework builder. *C. caespitosa* shows densely packed, thick dendroid corallites up to 30 cm long or loosely ramified colonies in life position (Stop 3) (Fig. 11). In some instances, fragmented colonies also occur. Coralligenous is sharply overlain by a progradational unit of bioclastic grainstone to rudstone (with grainstone matrix), several meters thick, described in detail by Zecchin et al. (2010), and including a clinostratified body nucleated around a tectonic step (normal fault stop 3 and 4). It is interpreted as a submerged spit fed by eastward directed longshore drift (Stop 3) (Fig. 12). The contact between the algal/coral build-ups and the bioclastic layers is sub-horizontal and only very localized evidence of erosional truncation occurs (Stop 3). In the other cases, it preserves irregular relief at the cm to dm scale.

Figure 10. The outer, southern Coralligenous discrete column and hybrid banks (red contour) of Le Castella, SE of the Aragonese castle. Note the thickness of the biocalcarenite layers at the top. Person as scale is 1,75 m tall.

Figure 11. *Clacodora caespitosa* with densely packed, thick dendroid corallites up to 30 cm, ramified colony in life position. Note the gray muddy sediment that turns to yellowish coarse sand and gravel at the top. Hammer as scale.

Figure 12. Le Castella clinostratified body outcropping in the southern sector of the Le Castella marine terrace, in front of the Aragonese castle. Scale bar is 1 m.

6. CAPO COLONNA MARINE TERRACE (5 September)

Capo Colonna marine terrace forms an approximately 2.5 km long, WE oriented, promontory of the Crotone peninsula. Morphologically, it consists of a planar surface gently inclined toward the E, with an elevation ranging between $\sim$ 65 m above sea level at the inner margin, and 10 m at its distal portion.

The mixed carbonate-siliciclastic sedimentary cover of the terrace is exposed quite continuously along the northern coast of the promontory, never exceeding 10 m of thickness, except in its proximal segment. The outcrops along the southern coast are more scattered. Shallow water marine biogenic carbonate facies, including extensive Coralligenous build-ups, are exceptionally well represented. The age of the Capo Colonna terrace has been correlated with Marine Isotope Stage 5.1, about 80 ka BP, by Infrared luminesce [45]; by aminostratigraphy [47]; by U/Th technique [48]; and by lithostratigraphy [49] (Fig. 4).

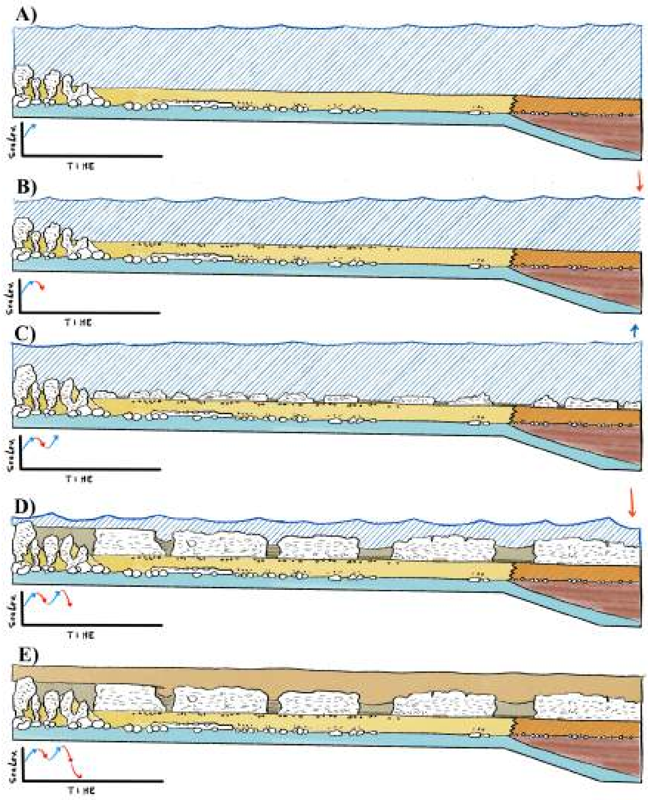

Figure 13. Interpretative scheme of the composite nature of the Capo Colonna marine terrace, with the development of different facies along the shelf within the upper, second high frequency transgressive–regressive cycle, revised from Bracchi et al. (2014). A) Late transgression and early highstand phase: Coralligenous develops in the proximal sector, sparse praline rhodoliths accumulate in the central sector, and a maerl bed starts to develop in the distal sector; B) possible higher frequency drop in base level, with development of a hardground marked by borings of *Gastrochaenolites lapidicus* in the central sector and accumulation of abraded rhodoliths at the top of the maerl bed in the distal sector; C) late highstand phase, characterized by Coralligenous growth and development along the entire shelf profile; D) early stage of the regression. Coralligenous build-ups in the inner sector are erosionally truncated under the development of a regressive surface of marine erosion, whereas Coralligenous continues growing in central and outer sectors; E) late stage of regression: Coralligenous is buried by shallow marine bioclastic sediments (today biocalcarenite). Due to the effect of tectonic regional uplift, the terrace deposits became subaerially exposed.

6.1. Sequence Stratigraphy

The composite nature of the Capo Colonna marine terrace is documented by the preservation of two high frequency transgressive–regressive cycles arranged in a retrogradational stacking pattern, within the Marine Isotope Stage 5a [2, 49, 50] (Fig. 13).

The deposits of the first, lower cycle are preserved only in the distal part of the promontory and consist of a very limited outcrop.

The second, upper cycle constitutes the majority of the Capo Colonna marine terrace deposits. It is strongly asymmetrical, with a condensed transgressive and a thicker regressive portion. During the transgressive phase, at the base of the second cycle, a basal conglomerate formed (Fig. 13A). Above, a skeletal packstone occurs in the central sector laterally corresponding to a maerl bed, which is preserved only in the most distal segment of the terrace (Fig. 13A). Coralligenous starts developing only in the proximal, inner sector of the shelf (Fig. 13A).

The top of the maerl bed can be laterally correlated with the hardground occurring in the central sector (Fig. 13B). The maerl bed is stratigraphically well constrained between the final phase of transgression and the early highstand, when deepest water conditions were attained on the Capo Colonna paleoshelf (Fig. 13B).

The inner sector was colonized by Coralligenous between the final phase of transgression and the early highstand, becoming the volumetrically most important facies all along the paleoshelf, from the final transgressive phase and during the highstand, until the regressive phase when burial occurs (Fig. 13C, D). Coralligenous directly overlies the rhodolith-bearing skeletal packstone and the maerl bed in the central and distal sectors, respectively. Proximal build-ups, on the other hand, directly encrust blocks of the basal conglomerate and are overlain by (and locally in lateral contact with) progradational deposits of the shore-connected clastic wedge (Fig. 13C, D). Proximal build-ups occurred very close to the inner margin and were the first to be affected by the regression (Fig. 13D, E), which then involved all the paleoshelf. Coralligenous is conformably overlain by shoreface calcarenites in proximal and distal settings (Fig. 13E). These calcarenites also marked the final burial of Coralligenous during regression. The submerged regressive surface, developed during regression in the median sector, erosionally truncates the calcarenite and the build-ups (Fig. 13E).

Figure 14. Dome to mushroom-like build-ups (red contour) of Capo Colonna proximal sector. Person as scale is 1,80 cm tall.

6.2. Coralligenous

The spectacular Pleistocene fossil algal build-ups observed along the paleoshelf of Capo Colonna marine terrace was previously described as algal boundstone, and recently detailed at the microscale as red algae bindstones, bryozoan boundstones and, serpulid boundstones. Bracchi et al. (2014) specifically focused on the analysis of the algal boundstone to give insights into the main features of algal build-ups and their evolution in the framework of the composite 5a eustatic cycle.

Figure 15. Coralligenous bank (red contour) of Capo Colonna central sector. Person as scale is 1,70 cm tall.

Figure 16. Detail of the borings of the ichnospecies *Gastrochaenolites lapidicus* from the hardground at the base of Coralligenous banks in the central sector of Capo colonna marine terrace. Hammer as scale.

Figure 17. Coralligenous small bank (red contour) of Capo Colonna outer sector. Note the thick maerl bed at the base (blue arrow). The light-blue line indicates the base of the maerl bed. Capo colonna has been recognized as a composite marine terrace with two cycles, and this outcrop includes at the base (light-blue arrow) the deposits of the transgressive phase of the first cycle. Person as scale is 1,80 cm tall.

The terrace can be divided into three sectors, from proximal to distal. The proximal sector records progradation of a shore-connected clastic wedge, with rare Coralligenous, in the form of irregular domes to mushroom-like build-ups (Fig. 14). These are hybrid banks, generally larger than higher, about 1 up to 3 m thick and never exceeding 5 m of lateral continuity, grown on a basal conglomerate. The singular build-up shows a massive core, with a dense framework, passing to a more cavernous structure in the external part, with the presence of up to 40 cm large, serpulid-lined pockets. These pockets have an irregular shape, and are filled by coarse yellowish sediment of both terrigenous and biogenic origin. The algal framework is generally dense with leafy laminar overgrowing crusts, alternating with micritic gray matrix. The direction of crust development is not homogeneous. They are parallel to the substrate at the base of the build-up, whereas they assume a different orientation, even perpendicular to the substrate, in its vertical and lateral development. Among build-ups, coarse mixed siliciclastic-biogenic packstone to grainstone occurs. Proximal build-ups had a relatively short time interval for their development, that, together with the spatial discontinuity of the basal conglomerate, were the main factors preventing the development of more continuous banks.

The central sector includes Coralligenous banks (Stop 1), together with skeletal packstone, grainstone, and rudstone, truncated by a regressive surface of marine erosion overlain by a shoreface calcarenite (Fig. 15). Interestingly, Coralligenous develops on a hardground, marked by the occurrence of *Gastrochaenolites lapidicus* (Fig. 16) (Stop 1), which represents a continuous, flat, hard substrate. Banks have a regular thickness of 3-4 m and tens of meters of lateral continuity in the WE direction. The inner morphology of the banks is very irregular because of numerous, dm-sized, round to columnar cavities filled by sediment, resulting in a locally cavernous structure. The algal framework is dense and matrix poor, with rare exceptions. Coralline algae grow laminar to leafy and form a layered fabric, but lumpy growth forms are locally dominant. Even in this case, the framework is complex and the algal crusts do not show a homogeneous growth direction from the bottom to the top.

The distal sector is fully dominated by biogenic deposits, with coralligenous bioconstructions and skeletal wackestone, packstone, and rudstone, where abundant rhodoliths occur (Fig. 17) (Stop 2). Coralligenous still forms banks, and the thickness ranges between 1 and 2 m. The distal Capo Colonna Coralligenous deposits fully conform to the definition of a fossil example of Coralligenous *de plateau*, due to the colonization and bounding of the rhodolith bed (maerl) that gave origin to the Coralligenous rigid framework (Basso et al., 2007).

The crustose coralline algae assemblages of proximal sector are mostly dominated at the base of the structures by *L. stictaeforme* and *Lithophyllum* sp. associated with bryozoans, whereas *M. alternans* becomes dominant at the top of the structures (Fig. 18) . Coralligenous in the central sector is formed by *M. alternans*, *Mesophyllum* sp., *L. minervae*, *Lithothamnion* sp., with *Mesophyllum* sp., *Lithophyllum* sp., and *Titanoderma* sp. becoming predominant at the top of the structures (Fig. 18) . In the distal sector, build-ups are mainly bioconstructed by *M. alternans* and *Mesophyllum* sp., with encrusting bryozoans being locally dominant at the top of the build-ups (Fig. 18).

6.3. Rhodoliths and maerl bed

Praline rhodoliths are found sparsely in a tabular bed of skeletal packstone directly underlying the Coralligenous of the central sector (Fig. 19) (Stop 1 or 2). These pralines form laterally discontinuous subhorizontal accumulations usually forming rhodolith rudstone pockets in the packstone. These pralines generally show a fruticose growth form, with protuberances up to 1-1.5 cm in length, with sometimes a lithic pebble as nucleus. Their shape varies between spheroid and discoid, 2-5 cm in diameter. The pralines are formed by several species of non-geniculate coralline algae, such as *Lithothamnion* sp., *Mesophyllum* sp. and rarely *Titanoderma pustulatum*. On the basis of their features, these pralines are interpreted as having formed in the infralittoral zone, under moderate to high hydrodynamic conditions.

A spectacular fossil maerl bed is preserved in the outer sector (Fig. 17) (Stop 2). This unit consists of a rudstone in which the grain supported structure is mostly formed by unattached red algae branches and fragments often coated by micritic rims, in a siliciclastic matrix. The laterally continuous bed is 40 to 60 cm in thickness and it overlies a thin amalgamated level of poorly sorted pebbly conglomerate rich in bioclasts. The conglomerate sets erosionally on the deposits of the first, lower Capo Colonna cycle (Fig. 17). The identified species are *Lithothamnion corallioides*, *Phymatolithon* sp., *Lithophyllum* sp. and *Lithothamnion* sp. Present-day Mediterranean maerl develops under moderate to high hydrodynamic conditions and/or low sedimentation rate, which prevent its burial. Light and salinity are considered two other environmental factors influencing the maerl distribution with an optimum depth range between 30 and 70 m wd for the Mediterranean Sea (Basso et al., 2016). Fossil maerl of Capo Colonna shows similar features and can be interpreted as a circalittoral facies, corresponding to the deeper deposits within the upper cycle. An estimated paleodepth of formation for the maerl bed can be inferred from the difference in elevation between the most proximal marine deposits at the base of the paleocliff at the inner margin ($\sim$50, 55 m above sea level) and the maerl bed ($\sim$10 m above sea level). The resulting value of $\sim$40-45 m is remarkably concordant with the depth optimum for the development of present-day Mediterranean maerl [42]. Finally, in the uppermost part of the maerl bed, a level of abraded praline

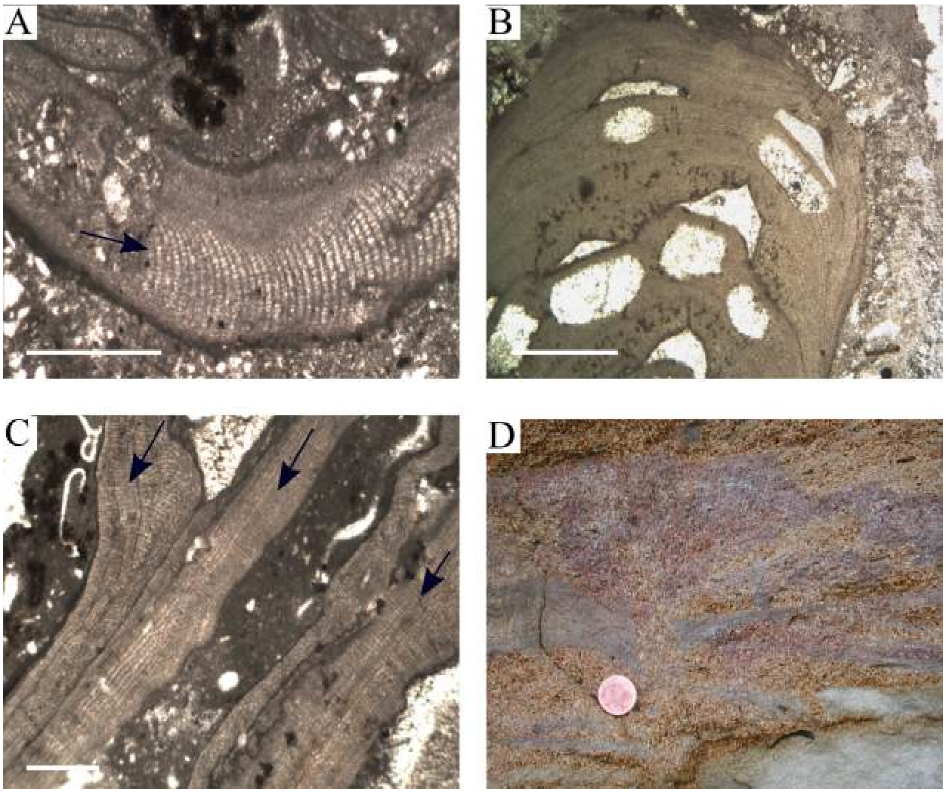

Figure 18. Crustose coralline algae and maerl facies identified in the Capo Colonna marine terrace deposits. A) *Mesophyllum*sp.: detail of the thallus with the thick coaxial hypothallus (black arrow); B) *Lithothamnion minervae*: the thallus includes some conceptacles with the typical triangular cavities at the top; C) *Lithophyllum* gr.*sticiforme*: foliose superposed thalli (black arrows) with the characteristic regular cell arrangement; D) field image of the maerl facies occurring in the distal portion of Capo Colonna marine terrace deposits. Scale bar in A-C is 500 µm.

rhodoliths has been observed. They show evidence of abrasion and erosion, in the form of strong flattening of their external surface. Remnants of the original fruticose growth form are detectable. These rhodoliths have diameters ranging between 3 and 7 cm, and are mostly formed by *Lithothamnion* sp.

Figure 19. Examples of the small sparse pralines rhodoliths occurring in the biogenic packstone and grainstone in the central and distal sectors of the Capo Colonna marine terrace.

6.4. Bio-sedimentary processes and role of micrite in the formation of calcareous algal bioconstructions and associated sediments

As seen, the skeletal primary framework of the algal buildups, consists of laminar to massive encrusting coralline red algae acting as main bioconstructors, with minor bryozoans, encrusting foraminifera, and serpulids as secondary frame-builders (Fig. 20A). Whereas, the autochthonous mäerl tabular beds are mainly composed of free-branched coralline red algae rudstone (Fig. 20B). Moreover, a variable amount of sandy bioclastic sediment is laterally interbedded with the bioconstructions and tends to be entrapped in their cavities and pockets (Fig. 20C).
All sedimentary sub-facies of the bioconstructions and associated sediment are rich in autochthonous syn-sedimentary microbial-mediated micrite, forming aphanitic, peloidal, clotted peloidal, and filamentous fabrics [51] (Fig. 20C-F). Microbial micrite can also trap and bind a variable amount of grains (Fig. 20C, E) , or be a secondary component of the sandy and bioclastic sediment as micritic rims surrounding the clasts (Fig. 20B). SEM views of all these early-lithified micrites show the typical nanostructure of the primary microbial-mediated carbonates, rather than a detrital mud particles accumulation, as they consist of nanospheres coalescing into subhedral microcrystals that replace both extracellular substances (Fig. 20G) and microbial cells (present with several morphological types) (Fig. 20H). This in turn implies the original widespread presence of benthic lithifying microbial biofilms, that colonized both the cavities of the skeletal framework of the bioconstructions, and the intergranular space of the associated sediment. These microbial communities, thanks to the metabolic processes of the microorganisms that induced the carbonate precipitation, significantly contributed to the early cementation of all the deposits.

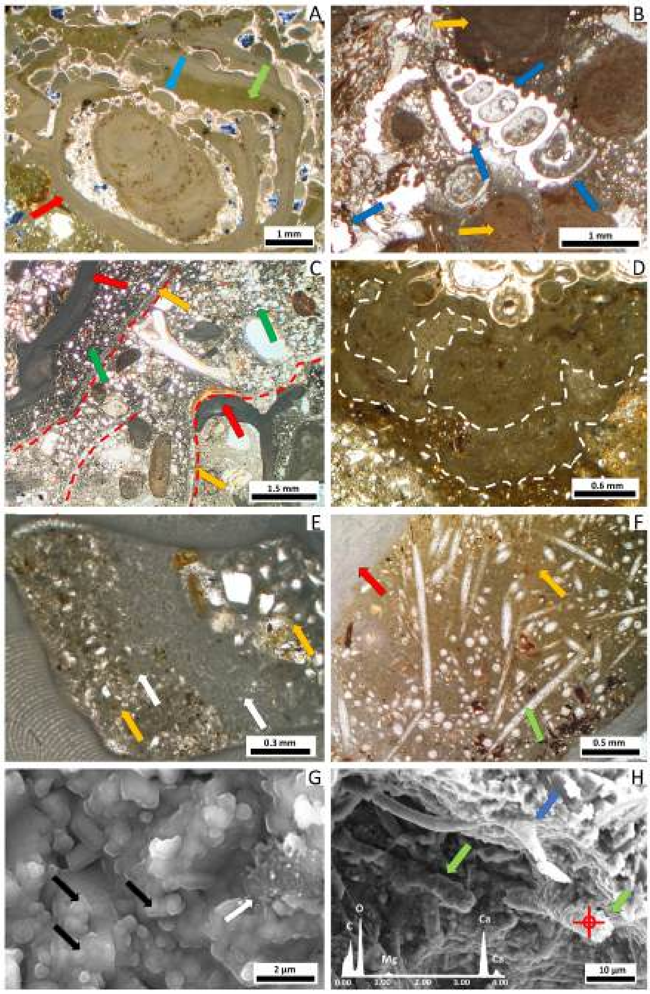

Figure 20. From Santagati et al. (2024): (A) Red algae bindstone (coralligenous facies): algal crusts (red arrow) with encrusting foraminifera (blue arrow) and micritic (green arrow) and microspar infill; (B) algal rudstone (mäerl facies): free red algae branches (yellow arrows), note micritic rims around “phantom” dissolved molluscs and bioclasts (blue arrows); (C) Microbialitic crusts (yellow arrows) with filamentous fabric, developed on erosive surfaces (red dashed lines) on algal thalli (red arrows) and associated bioclastic packstone sediment (green arrows); (D) Micro-mound microbialite (white dashed lines) developed in the algal boundstone with clotted peloidal fabric; (E) "Pure" peloidal micrite (white arrows) with trapped sediment (yellow arrows) filling a cavity between red algal thalli; (F) sponge spicules (green arrow) associated with clotted peloidal micrite (yellow arrow) between algal thalli (red arrow); (G) SEM image of micrite crystals ultrastructure composed of aggregates of nanospheres (black arrows). Note organic matter remains (white arrow) partially mineralized by the mineral nanospheres. (F) Cluster of filamentous bacterial bodies of different types (green and blue arrows) mineralized by nanospherical micrite; red point represents the spot of EDS analysis reported as spectrum.

6.5. References

1. Bracchi, V.A., Nalin, R., Basso, D. (2014). Paleoecology and dynamics of coralline-dominated facies during a Pleistocene transgressive–regressive cycle (Capo Colonna marine terrace, Southern Italy). *Palaeogeogr. Palaeoclimatol. Palaeoecol.*, 414, 296–309.
2. Bracchi, V. A., Nalin, R., and Basso, D. (2016). Morpho-structural heterogeneity of shallow-water coralligenous in a Pleistocene marine terrace (Le Castella, Italy). *Palaeogeogr. Palaeoclimatol. Palaeoecol.*, 454, 101–112.
3. Ballesteros, E. (2006). Mediterranean coralligenous assemblages: a synthesis of present knowledge. *Oceanogr. Mar. Biol. Annu. Rev.*, 44, 123–195.
4. Pérès, J.M., Picard, J. (1964). Nouveau manuel de bionomie benthique de la mer Méditerranée. *Recent Trav. Stat. Mar.*

Endoume, 31 (47), 1–137.
5. Pérès, J.M. (1982). Structure and dynamics of assemblages in the benthal. *Marine Ecology* 5(1), 119–185. In: *Marine ecology: a comprehensive, integrated treatise on life in oceans and coastal waters: 5. Ocean management Vol. 1* (Ed. Kinne O.), John Wiley and Sons Inc., 119–185.
6. Sarà, M. (1969). Research on coralligenous formations: problems and perspectives. *Pubbl. Stn. Zool. Napoli*, 37 (Suppl.), 124–134.
7. Sarà, M., Pulitzer-Finali, G. (1970). Nuove vedute sulla classificazione dei fondi coralligeni. *Pubbl. Stn. Zool. Napoli*, 38, 174–179.
8. Pansini, M., Pronzato, R. (1973). Il coralligeno di Bogliasco ed il suo popolamento di Poriferi. *Boll. Mus. Ist. Biol. Univ. Genova*, 41, 5–34.
9. Hong, J.S. (1980). Étude faunistique d'un fond de concrétionnement de type coralligène soumis à un gradient de pollution en Méditerranée nord-occidentale (Golfe de Fos). Thèse de Doctorat. Université d'Aix-Marseille II (134 pp.).
10. Laborel, J. (1987). Marine biogenic constructions in the Mediterranean: a review. *Sci. Rapp. Port Cros Natl. Park*, 13, 97–126.
11. Sartoretto, S. (1994). Structure et dynamique d'un nouveau type de bioconstruction à *Mesophyllum lichenoides* (Ellis) Lemoine (corallinales, rhodophyta). *C. R. Acad. Sci. III*, 317, 156–160.
12. Argenti, L., Taramelli, E., Matteucci, B., Argano, R. (1989). Notizie preliminari sui popolamenti vagili di formazioni coralligene infralitorali al largo di S. Severa (Roma). *Oebalia*, 15 (1), 287–288.
13. Chiocci, F.L., Chimenz Gusso, C., Celletti, G., Argenti, L., Di Geronimo et al. (2001). Possible biological origin of shallow-water shoals in a middle-latitude microtidal coast. *Biol. Mar. Mediterr.*, 8 (1), 216–222.
14. Bracchi, V.A., Basso, D., Marchese, F., Corselli, C., Savini, A. (2017). Coralligenous morphotypes on subhorizontal substrate: a new categorization. *Cont. Shelf Res.*, 144, 10-20.
15. Casas-Güell, E., Teixidó, N., Garrabou, J., Cebrian, E. (2015). Structure and biodiversity of coralligenous assemblages over broad spatial and temporal scales. *Mar. Biol.*, 162, 901–912.
16. Sartoretto, S., Schohn, T., Bianchi, C.N., Morri, C., Garrabou, J. et al. (2017). An integrated method to evaluate and monitor the conservation state of coralligenous habitats: the INDEX-COR approach. *Mar. Pollut. Bull.*, 120, 222-231.
17. Corriero, G., Pierri, C., Mercurio, M., Nonnis Marzano, C., Onen Tarantini et al. (2019). A Mediterranean Mesophotic Coral Reef Built by Non-symbiotic Scleractinians. *Sci. Rep.*, 9, 3601.
18. Gili, J.M., Ros, J. (1985). Study and cartography of the benthic communities of Medes islands (NE Spain). *P.S.Z.N.I. Mar. Ecol.*, 6 (3), 219–238.
19. Garrabou, J., Ballesteros, E., Zabala, M. (2002). Structure and dynamics of north-western Mediterranean rocky benthic communities along a depth gradient. *Estuar. Coast. Shelf Sci.*, 55, 493–508.
20. Di Geronimo, I., Di Geronimo, R., Rosso, A., Sanfilippo, R. (2002). Structural and taphonomic analyses of a columnar coralline algal build–up from SE Sicily. *Geobios*, 35 (1), 86–95.
21. Virgilio, M., Airoldi, L., and Abbiati, M. (2006). Spatial and temporal variations of assemblages in a Mediterranean coralligenous reef and relationships with surface orientation. *Coral reefs*, 25, 265–272.
22. Casellato, S., and Stefanon, A. (2008). Coralligenous habitat in the northern Adriatic Sea: An overview. *Mar. Ecol.*, 29, 321–341.
23. Ponti, M., Fava, F., and Abbiati, M. (2011). Spatial-temporal variability of epibenthic assemblages on subtidal biogenic reefs in the northern Adriatic Sea. *Mar. Biol.*, 158, 1447–1459.
24. Falace, A., Kaleb, S., Curiel, D., Miotti, C., Galli, G. et al. (2015). Calcareous bio-concretions in the northern Adriatic Sea: Habitat types, environmental factors that influence habitat distributions, and predictive modeling. *PLoS ONE*, 10, e0140931.
25. Çinar, M. E., Féral, J. P., Arvanitidis, C., David, R., Taşkin, E. et al. (2020). Coralligenous assemblages along their geographical distribution: Testing of concepts and implications for management. *Aquat. Conserv. Mar. Freshw. Ecosyst.*, 30, 1578–1594.
26. Laubier, L. (1966). Le coralligène des Albères: monographie biocénotique. *Ann. l'Institut Océanogr. Monaco*, 43, 139–316.
27. Rosso, A., Sanfilippo, R. (2009). The Contribution of Bryozoans and Serpuloideans to Coralligenous Concretions From SE Sicily. In: *UNEM-MAP-RAC/SPA, Proceedings of the First Symposium on the Coralligenous and Other Calcareous Bio-Concretions of the Mediterranean Sea, Tabarka*, 2009, pp. 123–128.
28. Boudouresque, C. F., Blanfuné, A., Harmelin-Vivien, M., Personnic, S., Ruitton, S. et al. (2017). Where seaweed forests meet animal forests: The examples of macroalgae in coral reefs and the mediterranean coralligenous ecosystem. In: *Marine animal forests*, (Eds. S. Rossi, L. Bramanti, A. Gori, and C. Orejas), Cham: Springer, 369-396.
29. De Jode, A., David, R., Haguenauer, A., Cahill, A. E., Erga, et al. (2019). From seascape ecology to population genomics and back. Spatial and ecological differentiation among cryptic species of the red algae *Lithophyllum stictiforme/L. cabiochiae*, main bioconstructors of coralligenous habitats. *Mol. Phylogenetics Evol.*, 137, 104–113.
30. Basso, D., Nalin, R., Massari, F. (2007). Genesis and composition of the Pleistocene Coralligène de plateau of the Cutro Terrace (Calabria, Southern Italy). *N. Jb. Geol. Paläont.*, 244/2, 73–182.
31. Basso, D., Bracchi, V.A., Bazzicalupo, P., Martini, M., Maspero, F. et al. (2022). Living coralligenous as geo-historical structure built by coralline algae. *Front. Earth Sci.*, 10.
32. Titschack, J., Nelson, C.S., Beck, T., Freiwald, A., Radtke, U. (2008). Sedimentary evolution of a late Pleistocene temperate red algal reef (Coralligène) on Rhodes, Greece: correlation with global sea–level fluctuations. *Sedimentology*, 55, 1747–1776.
33. Bracchi, V.A., Bazzicalupo, P., Fallati, L., Varzi, A.G., Savini, A. et al. (2022). The Main Builders of Mediterranean Coralligenous: 2D and 3D Quantitative Approaches for its identification. *Front. Earth Sci.*, 10.
34. Bellan–Santini, D., Lacaze, J.C., Poizat, C. (1994). Les biocénoses marines et littorales de Méditerranée, synthèse, menaces et perspectives. *Collection Patrimoines Naturels*. Secrétariat de la Faune et de la Flore/M.N.H.N. 19, pp. 1–246.
35. Cocito, S. (2004). Bioconstruction and biodiversity: their mutual influence. *Sci. Mar.*, 68, 137–144.
36. Novosel, M., Pozar-Domac, A., Pasaric, M. (2004). Diversity and distribution of the Bryozoa along underwater cliffs in the Adriatic Sea with special reference to thermal regime. *Mar. Ecol.* 25, 155–170.
37. Bosellini, A., Ginsbourg, R.N. (1971). Form and internal structure of recent algal nodules (rhodolites) from Bermuda. *J. Geol.*, 79, 669-682.
38. Ginsburg, R.N., Bosellini, A. (1973). Form and internal structure of recent algal nodules (Rhodolites) from Bermuda: a reply. *J. Geol.*, 81, 239–241.
39. Bosence, D.W.J. (1984). Description and classification of

rhodoliths (rhodoids, rhodolites). T.M. Peryt (Ed.), *Coated Grains* (1983), pp. 217-224.

40. Basso, D. (1998). Deep rhodolith distribution in the Pontian Islands, Italy: a model for the paleoecology of a temperate sea. *Palaeogeogr. Palaeoclimatol. Palaeoecol.*, 137 (1–2), 173–187.
41. Steneck, R.S. (1986). The ecology of coralline algal crusts: convergent patterns and adaptative strategies. *Annu. Rev. Ecol. Syst.*, 17, 273–303.
42. Basso, D., Babbini, L., Espla, A.A., Salomidi, M. (2016). Mediterranean Rhodolith Beds. In *Rhodolith/Maerl Beds: A Global Perspective*, (Eds. R. Riosmena-Rodriguez, W. Nelson, J. Aguirre), pp: 281-298, Springer.
43. Zecchin, M., Nalin, R., Roda, C. (2004). Raised Pleistocene marine terraces of the Crotone peninsula (Calabria, Southern Italy): facies analysis and organization of their deposits. *Sediment. Geol.*, 172, 165–185.
44. Mauz, B., Hassler, U. (2000). Luminescence chronology of late Pleistocene raised beaches on Southern Italy: new data on relative sea–level changes. *Mar. Geol.*, 170, 187–203.
45. Nalin, R., Lamothe, M., Auclair, M., Massari, F. (2020). Chronology of the marine terraces of the Crotone Peninsula (Calabria, southern Italy) by means of infrared-stimulated luminescence (IRSL). *Mar. Petrol. Geol.*, 122, 104645.
46. Gliozzi, E. (1987). I terrazzi marini del Pleistocene superiore della penisola di Crotone (Calabria). *Geol. Romana*, 26, 17-79.
47. Zecchin, M., Caffau, M., Civile, D., Roda, C. (2010). Anatomy of a late Pleistocene clinoformal sedimentary body (Le Castella, Calabria, Southern Italy): a case of prograding spit system? *Sediment. Geol.*, 223 (3–4), 291–309.
48. Belluomini, G., Gliozzi, E., Ruggieri, G., Branca, M., Delitala, L. (1988). First dates on the terraces of the Crotone Peninsula (Calabria, Southern Italy). *Boll. Soc. Geol. It.*, 107, 249–254.
49. Nalin, R., Massari, F. (2009). Facies and stratigraphic anatomy of a temperate carbonate sequence (capo colonna Terrace, late Pleistocene, Southern Italy). *J. Sediment. Res.*, 79 (4), 210–225.
50. Zecchin, M., Caffau, M., Civile, D., Roda, C. (2009). Facies and cycle architecture of a Pleistocene marine terrace (Crotone, southern Italy): a sedimentary response to late Quaternary, high-frequency glacio-eustatic changes. *Sediment. Geol.*, 216, 138–157.
51. Santagati, P., Guerrieri, S., Borrelli, M., Perri, E. (2024). Calcareous bioconstructions formation during the last interglacial (MIS 5) in the central Mediterranean: A consortium of algal, metazoan, and microbial framebuilders (Capo Colonna -Crotone basin -South Italy). *Mar. Petrol. Geol.*, 10.1016/j.marpetgeo.2024.106950.

7. COLD-SEEP SYSTEM OF BELCASTRO (6 September)

The seafloor seepage of hydrocarbon-rich fluids from marine sediments is a process widely documented both in modern and ancient depositional settings [1-6]. Diagnostic features, such as the widespread formation of authigenic carbonates (calcite, aragonite and dolomite), the presence of microbial consortia and chemosymbiotic macrofauna and the presence of free gas or gas hydrates at or near the seafloor, characterize these depositional environments, together with the development of a variety of seafloor features including low-relief carbonate pavements, pockmarks and mud volcanoes.
Fossil cold-seep systems have been documented along the Italian peninsula [6-10], especially in the Cenozoic successions of the Apennine Mountains, showing ages spanning from the Eocene [11] to the Serravallian–Tortonian [4, 7, 12] and also Messinian [6, 13]. These systems commonly show the presence of chemosymbiotic macrofauna dominated by *Lucina* clams, which are historically known in Italy with the informal lithostratigraphic name *'Calcari a Lucina'* [4, 7, 14]. This unit also outcrops in southern Italy, such as in Sicily and Calabria [4, 15], with this latter hosting one of the biggest fossil cold-seep systems ever documented [16] (Fig. 21).

7.1. Stratigraphy

The stratigraphic framework in which the fossil cold-seep system is hosted is quite complicated, and still has some incertitude. In particular, the sedimentary succession starts with an alternation of conglomerates and massive arenites, accounting for a thickness of ca 20 m, directly overlying the crystalline basement. These deposits are attributed to the Serravallian/Tortonian San Nicola Formation, based on stratigraphic position and sedimentary affinity. Generally, the San Nicola Formation is characterized by a transgressive trend from clastic continental (fluvial–alluvial) to shallow marine facies (delta-front, intertidal and shoreface settings) [17-19] culminating in the Late Tortonian/Early Messinian with the deposition of the deeper marine claystones and marls of the Ponda Formation and the diatomites of the Tripoli Formation before the deposition of the Messinian evaporite-bearing deposits of the Petilia Policastro Formation [19, 20]. In Belcastro, both the Ponda and Tripoli Formations are missing, so the San NicolaFormation is directly in tectonic contact with the Petilia Policastro Formation [16]. Consequently, the presence of the Messinian Petilia Policastro Formation implies that an erosional event must have occurred no later than the Messinian. During this time interval the most pronounced and widespread erosive event was caused by the mid-Messinian sea-level fall, responsible for the formation of the regional Messinian Erosional Surface [e.g. 20], which in the studied succession corresponds to the erosional surface present at the top of the arenites and conglomerates, and consequently limiting upward the San Nicola Formation. After the Messinian sea-level drop, the Belcastro area remained under subaerial conditions up to the Pliocene, when the reflooding of the Mediterranean restored normal marine conditions in the entire Crotone Basin during the Zanclean [20]. This reflooding is testified by the deposition of a shelf-to-slope clay and silt of the Cavalieri Marls Formation [18, 19]. Upward the Cavalieri Marls Fm. is overlain by similar claystones rich in planktonic and benthic foraminifera with calcareous nannofossil, Piacenzian to mid Pleistocene in age, named Cutro Clay Formation.
Considering the possible thermal history of the Crotone Basin and the stratigraphic location of the possible source rock, the cold-seep carbonates most probably formed during the Pliocene (lateral to the Zanclean Cavalieri Marls Formation) in a fully marine environmental setting.

7.2. Cold-seep system of Belcastro

At least two Pliocene seep-related authigenic carbonate systems occur in Belcastro, within the Crotone Basin (North Calabria – Southern Italy) (Fig. 21). The southernmost mound-like carbonate body has a length of ca 350 m, a width of ca 100 to 150 m and a thickness of ca 40 m, being a very rare large outcrop, since the majority of cold-seep deposits are generally smaller. This carbonate body is characterized by a complex network of fractures and

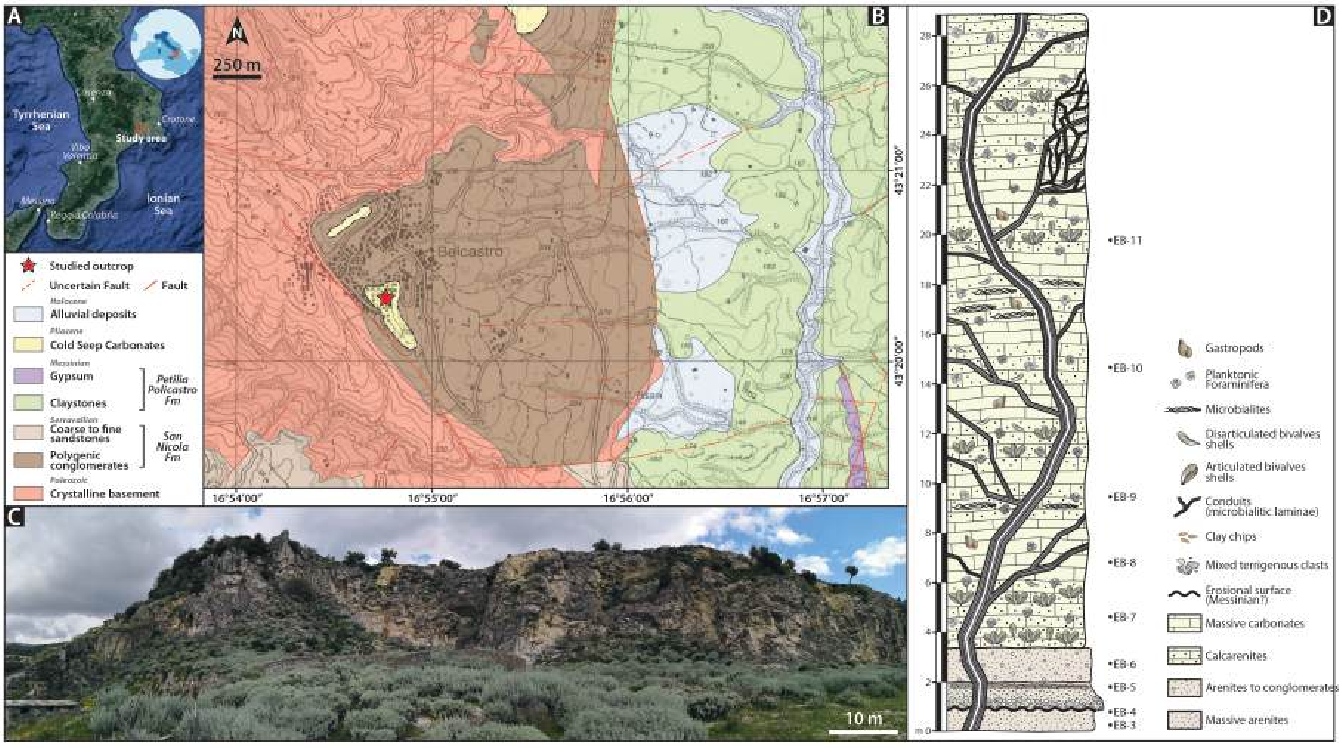

Figure 21. From Perri et al. (2024): geographic location (A) and geological map (B) of the study area; C) panorama view of the studied cold seep carbonate outcrop; D) measured sedimentary log and position of the samples of the cold seep carbonates outcropping in the quarry front of Belcastro.

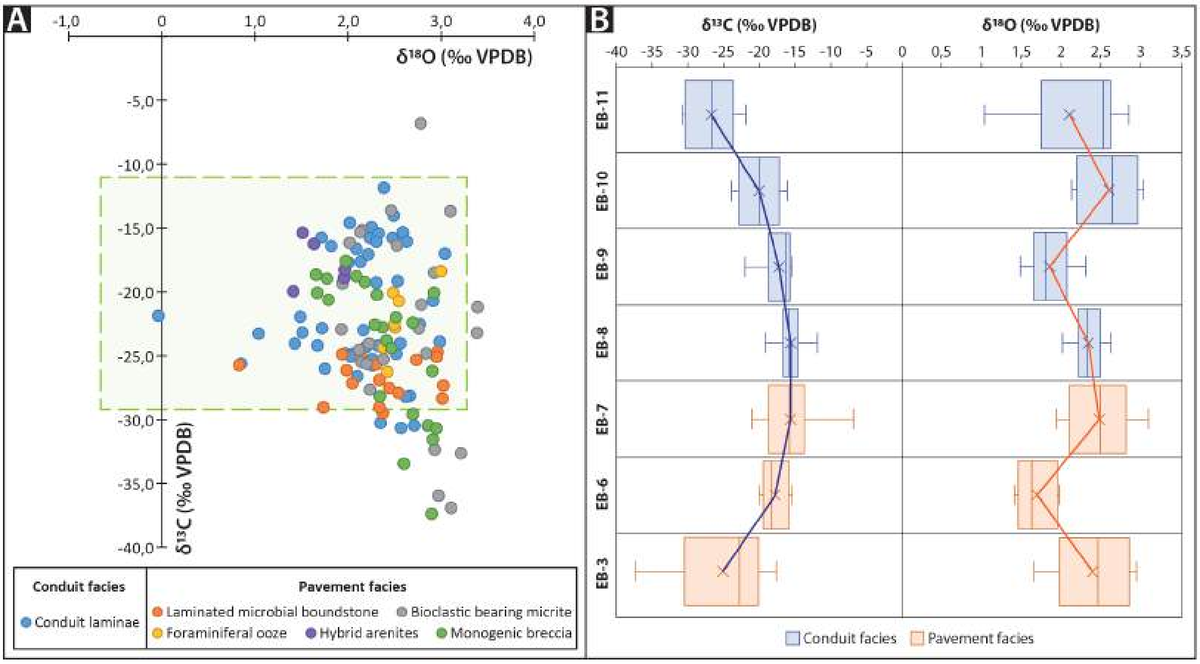

Figure 22. A) $\delta^{13}C$ and $\delta^{18}O$ isotopic composition of all microfacies forming the conduit and pavement facies. The green box represents the isotopic signature of modern seep carbonates in the Crotone Basin defined by Loher et al. (2018); B) Whisker plots highlighting the $\delta^{13}C$ and $\delta^{18}O$ variation along the stratigraphic succession showed in Fig. 21, with EB-3 representing the base and EB-11 the top of the succession. The continuous lines connect the average values. The orange boxes represent samples of the pavement facies, whereas the blue boxes represent samples of the conduit facies.

conduits through the fossil seafloor sediment that represent main flow-path for migrating hydrocarbons that contributed to the formation of authigenic carbonates both in the conduits and through the hosting sediments, forming lithified crusts (pavements) around the seepage area.

In analogy with most of the modern cold seeps [22, 23], the moderate $\delta^{13}C$ depletion of the studied deposits ($\delta^{13}C$ values between -6.8 ‰ and -37.4 ‰) probably accounts for thermogenic methane as dominant source, possibly mixed with carbon derived from marine dissolved inorganic carbon (DIC), or from the remineralization of organic matter, or heavier hydrocarbons [6, 23, 24] (Fig. 22). This interpretation is strengthened by numerous seepage sites and mud volcanoes in the nowadays offshore area of the Crotone Basin, where the same interpretation with regard to the hydrocarbon sources was provided [e.g. 3, 25] (Fig. 22).

In the studied deposits, the diagenetic effects seem negligible and the $\delta^{18}O$ values are generally positive, ranging between 0.0 ‰ to 3.4 ‰, and varying along the stratigraphic section from 1.7 ‰ to 3.0 ‰ in average (Fig. 22B). The generally positive values can be related to multiple and different processes occurring during carbonate precipitation such as the decomposition of gas hydrates, higher temperature fluid-rock interaction, clay mineral dehydration, changes in pH [e.g. 1, 26-28]. Among all these possibilities, the clay mineral dehydration may represent one of the dominant processes since different clay-dominated units were already buried at great depths during the cold seep system development, thus prone for dehydration.

Numerous previous studies on fossil and modern seeps indicated that the microbial communities are composed of a consortium of methanotrophic archaea and sulphate-reducing bacteria which thrive under anoxic conditions [e.g. 5, 28-30]. However, some fossil cold-seep authigenic carbonates have also been inferred to develop in oxygenated bottom waters along the Italian peninsula [4, 6, 10, 12, 14] on the bases of the widespread presence of chemosymbiotic *Lucina* clams and by the observation of predation holes in their shells caused by oxygen-dependent predators and grazers, such as crustaceans [e.g. 31-33].

In Belcastro, a precise taxonomic classification of the macrofauna is hampered due to bad shell preservation, dissolution and/or recrystallization. However, the few visible morphological characters of the shells suggest that they possibly belong to Lucinid and Solemyid groups that commonly colonize these particular environments. Moreover, the presence of also fecal pellets and common bioturbation structures, generally, but not exclusively, associated with oxygen-dependent macrofauna, together with the absence of pyrite, further suggest that the Belcastro cold-seep system possibly developed in oxygenated bottom waters or in oxygenated bottom waters only sometimes affected by limited periods of anoxia. In such kind of environment, the inferred consortium of SRB and methanotrophic archaea, as testified by the widespread occurrence of microbial boundstones and micritized microbial filaments (10 to 30 μm diameter and up to 1 mm length), was probably confined to the anoxic zone within the sediment column or, alternatively, to the lower part of a stratified microbial mat located at the seafloor and composed in its upper part of filamentous sulfide-oxidizing bacteria (SOB). In particular, the microbial boundstones probably formed very close to the main zones of methane leaks and greatly contributed to the early-cementation of the sediments and to the consequent formation of consolidated pavements, as testified to by the common presence of conduits fracturing the boundstones (Fig. 23). The pavements show a great lateral variability probably due to the different mechanisms of methane migration as diffusive flow and/or concentrated along the main conduits. In fact, away from the conduits, microbial mats were associated with the chemosymbiotic–bivalves packstone microfacies, made by chemosymbiotic (bivalves, shells remains) and non-chemosymbiotic (gastropods, crustaceans) organisms (Fig. 23). Planktonic foraminifera are ubiquitous in the pavement. They are generally dispersed within an aphanitic to clotted micrite matrix, or be associated with macrofaunal bioclasts in the chemosymbiotic–bivalves packstone, or represent the exclusive bioclastic component of the sediment, forming foraminiferal packstone/wackestone. In this latter case, the exclusive presence of unbroken foraminifera tests permits to infer a sedimentation mechanism due to pelagic rain from the water column, further indicating that this sedimentary facies formed a little bit further away from the methane emission sites. Moreover,

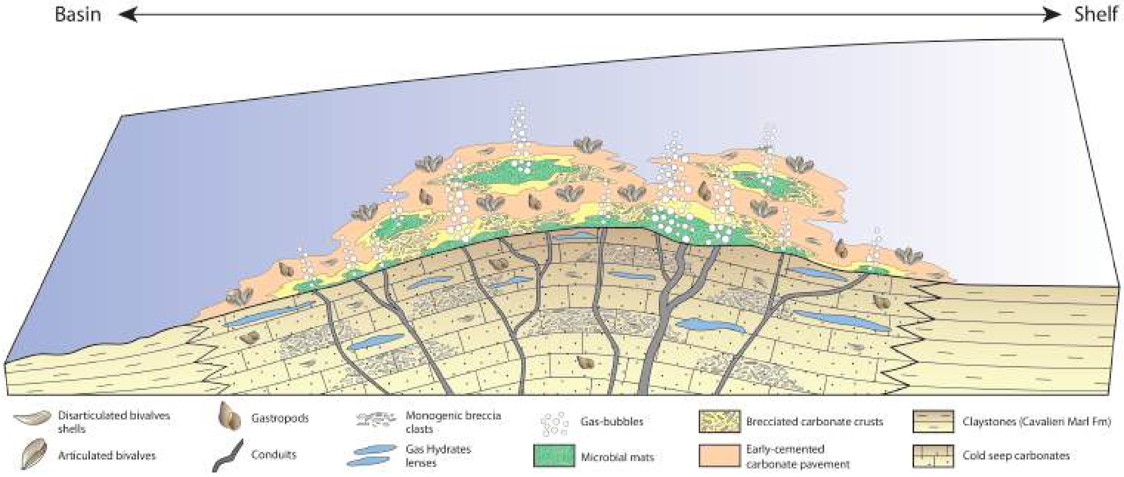

Figure 23. From Perri et al. (2024): idealized scheme of the Belcastro cold-seep system.

if not exclusive, the dominant presence of planktonic foraminifera also testifies that the cold-seep setting developed in a relatively deep-water environment.

7.3. The sedimentary facies of the cold-seep system of Belcastro

The sedimentary structures and biotic components of the carbonate system permit definition of two dominant sedimentary facies: (i) conduit facies; and (ii) pavement facies.

The conduit facies is characterized by a system of cavities and/or fractures with diameters from few centimeters up to 1 m, randomly cross-cutting the sediments and filled by multi-generational carbonate cements forming inward-accreted millimeter-thick laminae. The resulting network of conduits is very complex. The conduit facies is formed by the inward accretion of multiple generations of carbonate laminae. These laminae may completely fill the voids/channels or leave empty spaces in their innermost parts, subsequently filled by detrital sediments. The lamination pattern is formed by the alternation of dark micrite and clear sparite laminae. The micritic laminae are commonly typified by peloidal to aphanitic micrite forming flat to domal shaped laminae. The micrite is composed of sub-spherical nanocrystals commonly enveloped and/or surrounded by very thin clay mineral films and patches. Moreover, relicts of organic matter can occur. The sparite forming the light laminae varies from prismatic to pyramidal isopachous crystals to mosaics of anhedral to subhedral crystals. These crystals commonly show the presence of internal small-scale squared voids or larger voids following the crystal growth pattern (Fig. 24).

The pavement facies is commonly characterized by decimeter to meter-thick strata composed of laminated microbial carbonates (=boundstone) and of calcarenites with abundant macro- and microfossils. Bivalve shells (Lucinids) are abundant and generally preserved in life position forming fan-arranged clusters, although often dissolved or recrystallized with only external or internal mould remnants. In addition, disarticulated shells, gastropods and foraminifera are observed.

Five different microfacies types in the pavement facies have been identified: 1) laminated microbial boundstone, 2) chemosymbiotic–bivalves packstone, 3) foraminiferal packstone/wackestone, 4) hybrid arenites and 5) monogenic breccia.

1. *Laminated microbial boundstone* shows a well-laminated planar accreting pattern made by micritic–microsparitic to sparitic laminae alternations often cross-cut by multi-scale conduits (Fig. 25A). The micritic laminae are typified by thrombolitic to stromatolitic fabric composed of clotted to aphanitic, more rarely dendrolitic, micrite frequently incorporating planktonic foraminifera, bioclasts and micrite clasts (Fig. 25B). Spherical to oval peloids attributable to faecal pellets are observed regularly. In contrast, the sparitic laminae are characterized by microsparitic to sparitic (rarely prismatic) crystals forming isopachous laminae (Fig. 25C). Micritized filaments, commonly include dark organic matter residues, made of straight to curved unbranched individuals and with uniform thickness, are widespread and are encased within both micrite and sparite crystals (Fig. 25D, E). Traces of bioturbation occur as filled cavities, often showing an isopachous rim and an internal mosaic of sparite.
2. *Chemosymbiotic–bivalves packstone* is characterized by various bioclasts (bivalve shells, gastropods and serpulid/vermetid remains) dispersed within a micrite matrix (Fig. 25F). The matrix shows different and randomly organized fabrics composed of peloidal clotted and aphanitic micrite with occasional abundant dispersed planktonic foraminifera (Fig. 25G). Common bioturbation traces are filled with sparry calcite (Fig. 25G, H). Rare terrigenous grains occur.
3. *Foraminiferal packstone/wackestone* includes abundant planktonic foraminifera tests dispersed within a homogenous aphanitic micrite matrix and/or partly surrounded by microsparite (Fig. 26A). Rare siliciclastic detrital grains occur, together with fragmented bivalve shells and terrigenous clasts. Traces of bioturbation occur as cavities filled by sparite (Fig. 26B).
4. *Hybrid arenites* are characterized by abundant poorly sorted siliciclastic clasts including quartz, microcline, plagioclase, plutonic rock fragments, biotite, and subordinate garnet, titanite and green tourmaline surrounded by peloidal micrite and sparry calcite. Rarely, planktonic foraminifera tests occur (Fig. 26C, D). The hybrid arenites generally form localized centimeter-thick horizontal laminae alternating with the other carbonate microfacies and commonly show a good lateral continuity.
5. *Monogenic breccia* is characterized by angular to sub-angular, millimeter-sized clasts with edges that often fit together, cemented by microsparitic calcite, aphanitic to clotted micrite, aphanitic micrite or by acicular rimming cement passing to sparry calcite mosaic (Fig. 26E, F). This facies does not show any evidence of clasts transport that, instead, almost fit together (Fig. 26G, H), testifying the *in situ* nature and a poorly energetic leakage/outburst of the pressurized hydrocarbons.

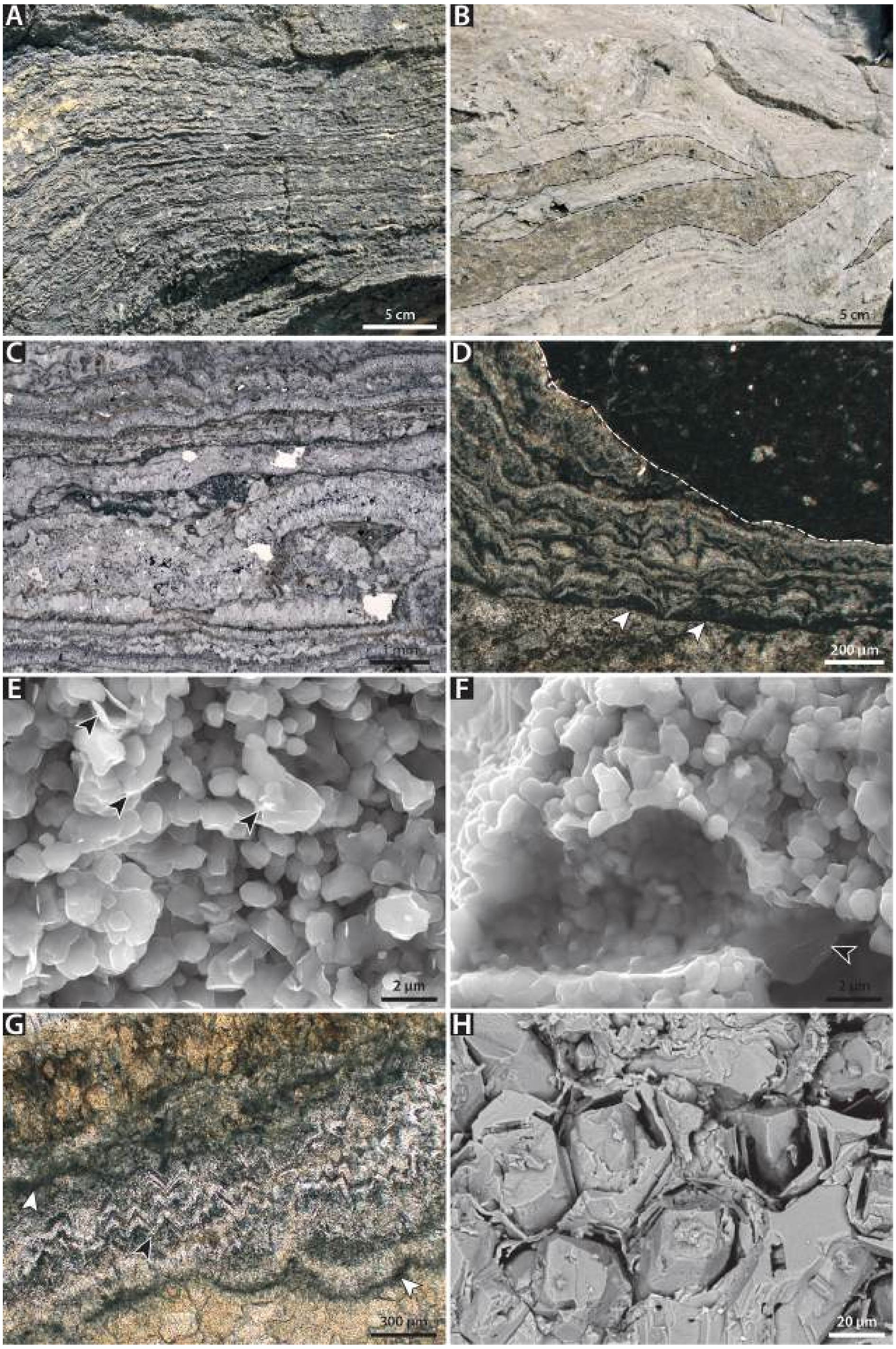

Figure 24. From Perri et al. (2024): main textural and sedimentological features of the conduit facies. A) Outcrop view of the carbonate laminae characterizing the conduit facies. B) Accreting carbonate laminae partially filling a conduit and isolating an internal void (black dashed lines), subsequently filled by detrital sediments. C) Typical petrographic aspect of the micritic and sparitic carbonate laminae alternation forming the conduit laminae microfacies. D) Micritic and microsparitic to sparitic laminae alternation. The micritic laminae show a microbial fabric forming flat to domal shaped laminae (white arrows) partially encrusting (dashed white line) a conduit which is filled by aphanitic peloidal to aphanitic micrite. E) SEM image of a micritic lamina showing the aggregation of sub-rounded to sub-squared nanocrystals commonly enveloped and/or surrounded by clay mineral patches (black arrows). F) Organic matter relict (black arrow) within a micritic lamina. G) Sparitic laminae alternating with thin apahanitic micrite laminae (white arrow), showing a prismatic to pyramidal isopachous texture (black arrow). H) SEM images showing sparry carbonate crystals of the sparitic laminae showing the common presence of intracrystalline voids following the crystallographic growth pattern of the crystals.

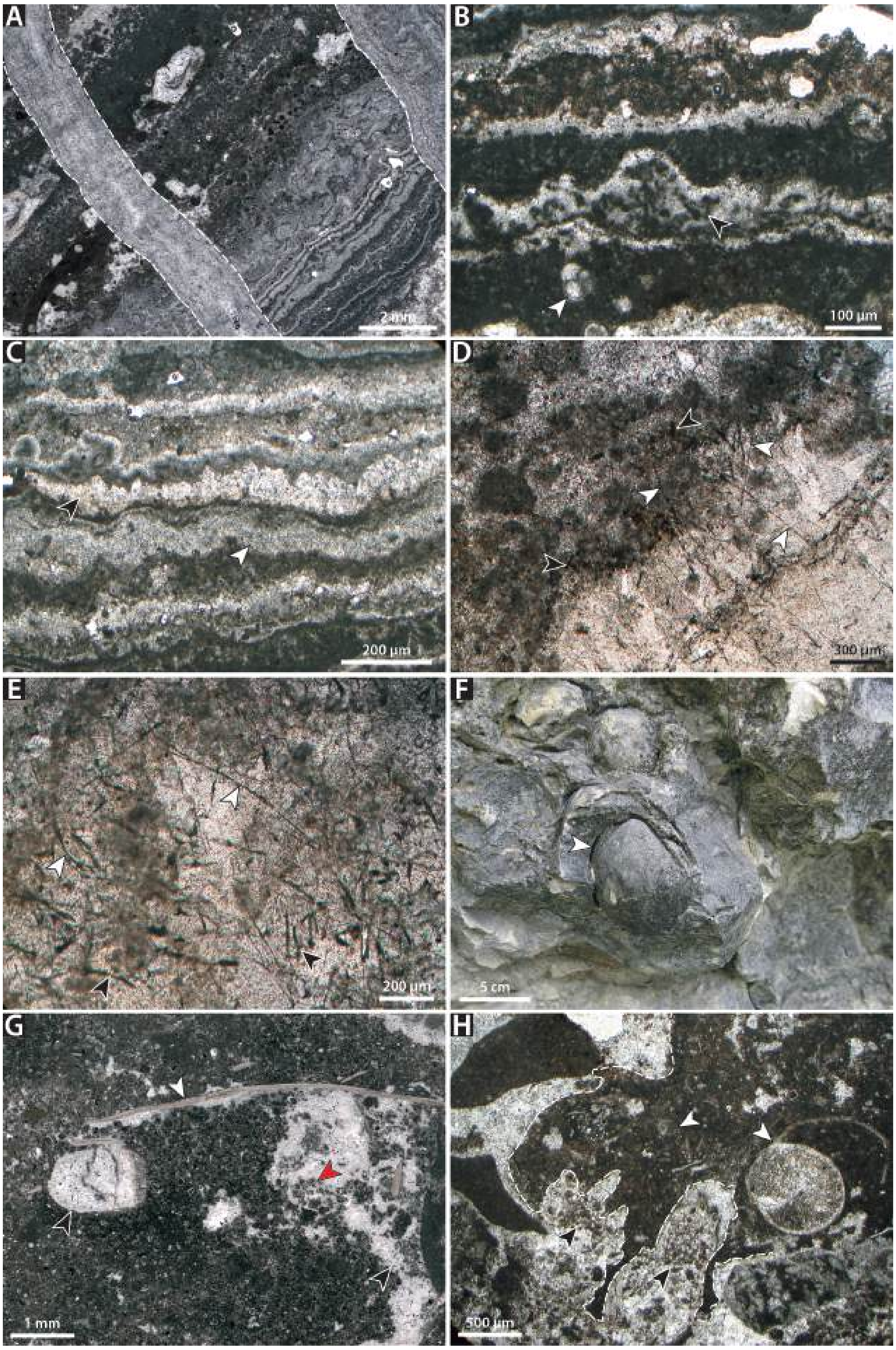

Figure 25. From Perri et al. (2024): photomicrographs illustrating the main textural features of the microbial boundstones microfacies. A) Laminated microbial boundstone formed by the alternation of micritic and microsparitic to sparitic laminae crosscut by small-scale conduits (outlined by stippled white line). Note the different textures of the conduit laminae and the microbial boundstone laminae. B) Close-up view of micritic laminae characterized by a dendrolithic (white arrow) and peloidal fabric incorporating planktonic foraminifera (black arrow). C) Close-up view of sparitic laminae composed of both, isopachous crusts of calcite crystals (black arrow) and microsparitic calcite (white arrow). D) Long and thin Filaments crossing both the sparite and micrite (white arrows). Within the micrite shot and thick filaments also occur (black arrows). E) Long and thin (white arrows) and short and thick (black arrows) filaments with a curved morphology. F) Outcrop image showing a dissolved bivalve shell (white arrow) in the chemosymbiotic bivalves packstone microfacies. B) Bivalve shell (white arrow) embedded within aphanitic micrite containing abundant planktonic foraminifera tests. Bioturbation traces (black arrows) are commonly filled with sparry calcite, in places showing the presence of clotted micrite (red arrow). H) Irregular bioturbation traces (white dashed line) are generally filled by sparitic to microsparitic calcite with dispersed clotted micrite (black arrows). Note the presence of gastropods shells (white arrows) within the mostly aphanitic micrite.

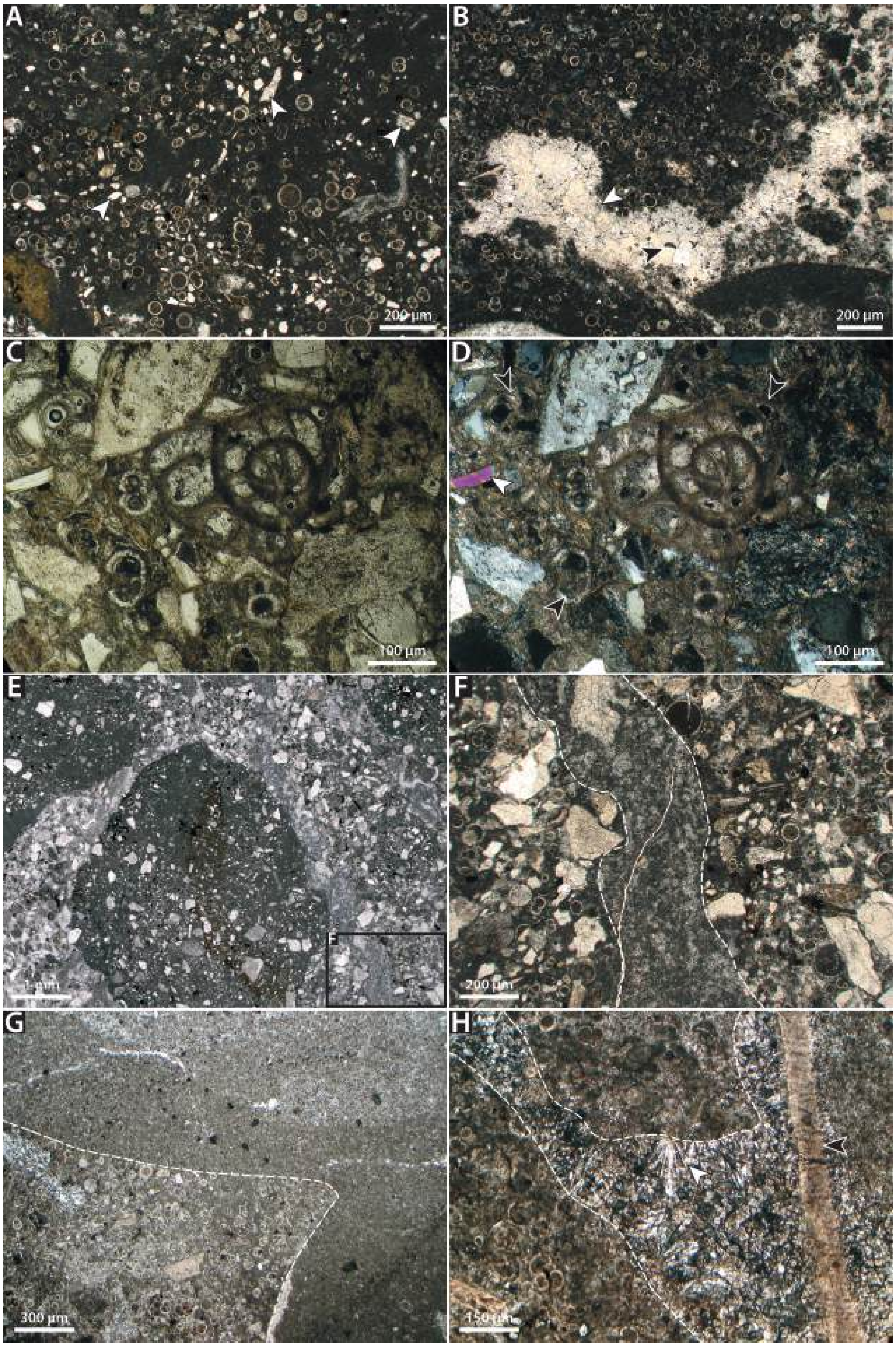

Figure 26. From Perri et al. (2024): photomicrographs illustrating the main features of the foraminiferal packstone/wackestone, hybrid arenites and monogenic breccia microfacies type. A) Abundant planktonic foraminifera tests are embedded within a homogenous aphanitic micrite matrix. Terrigenous clasts occur sporadically (white arrow). B) Cavities caused by bioturbation traces are highlighted by sparite fillings exhibiting an isopachous rim (white arrow) and a drusy sparite mosaic (black arrow). The sparite filling commonly incorporates clotted micrite, foraminifera tests and/or detrital clasts. C, D) Coeval carbonate intrabasinal grains (CI of Zuffa, 1980) of planktonic foraminifera (black arrows) mixed with silicic clastic contribution such as muscovite (white arrow), quartz, plagioclase and metamorphic lithic grains. E) Photomicrographs illustrating the main features of the. E) Typical aspect of the monogenic breccia composed of angular clasts, (here hybrid arenites), with edges that in some parts almost fit together. F) Close-up view of two individual breccia clast edges (white dashed lines) cemented by clotted micrite and microsparite. G) Angular breccia clast of the foraminiferal packstone/wackestone microfacies (white dashed line) surrounded by aphanitic micrite matrix. H) Foraminiferal packstone/wackestone microfacies breccia clasts (white dashed lines) and an isolated bivalve shell (black arrow) cemented by acicular calcite (white arrow).

7.4. References

1. Aloisi, G., Pierre, C., Rouchy, J.-M., Foucher, J.P., Woodside, et al. (2000). Methane-related authigenic carbonates of eastern Mediterranean Sea mud volcanoes and their possible relation to gas hydrate destabilisation. *Earth Planet Sci. Lett.*, 184, 321–338.
2. Pierre, C., Demange, J., Blanc-Valleron, M.M., Dupré, S. (2017). Authigenic carbonate mounds from active methane seeps on the southern Aquitaine Shelf (Bay of Biscay, France): Evidence for anaerobic oxidation of biogenic methane and submarine groundwater discharge during formation. *Cont. shelf Res.*, 133, 13–25.
3. Loher, M., Marcon, Y., Pape, T., Römer, M., Wintersteller, P., et al. (2018). Seafloor sealing, doming, and collapse associated with gas seeps and authigenic carbonate structures at Venere mud volcano, Central Mediterranean. *Deep-Sea Res. Part I*, 137, 76–96.
4. Taviani, M. (2001). Fluid venting and associated processes. In: Anatomy of an Orogen: The Apennines and Adjacent Mediterranean Basins (Ed. G.B. Vai), Springer, Netherlands, pp. 351–366.
5. Peckmann, J., Thiel, V. (2004). Carbon cycling at ancient methane–seeps. *Chem. Geol.*, 205, 443–467.
6. Natalicchio, M., Dela Pierre, F., Clari, P., Birgel, D., Cavagna, S., et al. (2013). Hydrocarbon seepage during the Messinian salinity crisis in the Tertiary Piedmont Basin (NW Italy). *Palaeogeogr. Palaeoclimatol. Palaeoecol.*, 390, 68–80.
7. Taviani, M. (1994). The "calcari a Lucina" macrofauna reconsidered: deep-sea faunal oases from Miocene-age cold vents in the Romagna Apennine, Italy. *Geo-Mar. Lett.*, 14, 185–191.
8. Natalicchio, M., Peckmann, J., Birgel, D., Kiel, S. (2015). Seep deposits from northern Istria, Croatia: a first glimpse into the Eocene seep fauna of the Tethys region. *Geol. Mag.*, 152, 444–459.
9. Argentino, C., Conti, S., Fioroni, C., Fontana, D. (2019a). Evidences for paleo-gas hydrate occurrence: what we can infer for the Miocene of the Northern Apennines (Italy). *Geosciences*, 9, 134.
10. Argentino, C., Conti, S., Crutchley, G.J., Fioroni, C., Fontana, D. et al. (2019b). Methane-derived authigenic carbonates on accretionary ridges: Miocene case studies in the northern Apennines (Italy) compared with modern submarine counterparts. *Mar. Petrol. Geol.*, 102, 860–872.
11. Venturini, S., Selmo, E., Tarlao, A., Tunis, G. (1998). Fossiliferous methanogenic limestones in the Eocene flysch of Istria (Croatia). *Giorn. Geol.*, 60, 219–234.
12. Taviani, M. (2001). Fluid venting and associated processes. In: Anatomy of an Orogen: The Apennines and Adjacent Mediterranean Basins (Ed G.B. Vai), Springer, Netherlands, 351–366.
13. Taviani, M. (2011). The deep-sea chemoautotroph microbial world as experienced by the Mediterranean metazoans through time. In: Advances in Stromatolite Geobiology (Eds J. Reitner, N.V. Queric and G. Arp), Lecture Notes in Earth Sciences, Springer-Verlag, Berlin, Germany, 131, 277–295.
14. Conti, S., Fioroni, C., Serventi, P., Fontana, D. (2022). Messinian seep-carbonates marking the transition to the evaporite deposits in the Romagna sector of the northern Apennines (Italy). *Ital. J. Geosci.*, 141, 350–362.
15. Ricci Lucchi, F., Vai, G.B. (1994). A stratigraphic and tectonofacies framework of the "calcari a Lucina" in the Apennine Chain, Italy. *Geo-Mar. Lett.*, 14, 210–218.
16. Borrelli, M., Umbro, B.F., Heimhofer, U., Santagati, P., Le Pera, E. et al. (2023b). Neogene cold seep carbonates in the Crotone Basin (South Italy). *Rend. Online Soc. Geol. It.*, 59, 2–8.
17. Perri, E., Borrelli, M., Heimhofer, U., Umbro, B., Santagati, P., et al. (2024). Microbial dominated Ca-carbonates in a giant Pliocene cold-seep system (Crotone Basin – South Italy). *Sedimentology*. doi: 10.1111/sed.13192
18. Massari, F., Prosser, G., Capraro, L., Fornaciari, E., Consolaro, C. (2010). A revision of the stratigraphy and geology of the south-western part of the Crotone Basin (South Italy). *Ital. J. Geosci.*, 129, 353–384.
19. Massari, F., Prosser, G. (2013). Late Cenozoic tectono-stratigraphic sequences of the Crotone basin; insights on the geodynamic history of the Calabrian Arc and Tyrrhenian sea. *Basin Res.*, 25, 26–51.
20. Zecchin, M., Civile, D., Caffau, M., Critelli, S., Muto, F., et al. (2020). Sedimentary evolution of the Neogene-Quaternary Crotone Basin (Southern Italy) and relationships with large-scale tectonics: a sequence stratigraphic approach. *Mar. Petrol. Geol.*, 117, 104381.
21. Borrelli, M., Perri, E., Avagliano, D., Coraggio, F., Critelli, S. (2022). Paleogeographic and sedimentary evolution of North Calabrian basins during the Messinian Salinity Crisis (South Italy). *Mar. Petrol. Geol.*, 141, 105726.
22. Roberts, H.H., Aharon, P. (1994). Hydrocarbon-derived carbonate buildups of the northern Gulf of Mexico continental slope: A review of submersible investigations. *Geo-Marine Letters*, 14, 135-148.
23. Loher, M., Marcon, Y., Pape, T., Römer, M., Wintersteller, P., et al. (2018). Seafloor sealing, doming, and collapse associated with gas seeps and authigenic carbonate structures at Venere mud volcano, Central Mediterranean. *Deep-Sea Res. Part I*, 137, 76–96.
24. Smrzka, D., Zwicker, J., Misch, D., Walkner, C., Gier, S., et al. (2019). Oil seepage and carbonate formation: a case study from the southern Gulf of Mexico. *Sedimentology*, 66, 2318–2353.
25. Ceramicola, S., Praeg, D., Cova, A., Accettella, D., Zecchin, M. (2014). Seafloor distribution and last glacial to postglacial activity of mud volcanoes on the Calabrian accretionary prism, Ionian Sea. *Geo-Mar. Lett.*, 34 (2), 111-129.
26. Aloisi, G., Bouloubassi, I., Heijs, S.K., Pancost, R.D., Pierre, C., et al. (2002). CH4-consuming microorganisms and the formation of carbonate crusts at cold seeps. *Earth Planet. Sci. Lett.*, 203, 195-203.
27. Greinert, J., Bollwerk, S.M., Derkachev, A., Bohrmann, G., Suess, E. (2001). Massive barite deposits and carbonate mineralization in the Derugin Basin, Sea of Okhotsk: precipitation processes at cold seep sites. *Earth Planet. Sci. Lett.*, 203, 165-180.
28. Teichert, B., Bohrmann, G., Suess, E. (2005). Chemoherms on Hydrate Ridge—unique microbially-mediated carbonate build-ups growing into the water column. *Palaeogeogr. Palaeoclimatol. Palaeoecol.*, 227, 67–85.
29. Boetius, A., Ravenschlag, K., Schubert, C.J., Rickert, D., Widdel, F., et al. (2000). A marine microbial consortium apparently mediating anaerobic oxidation of methane. *Nature*, 407, 623–626.
30. Taviani, M., Franchi, F., Angeletti, L., Correggiari, A., Lopez-Correa, M., et al. (2015). Biodetrital carbonates on the Adriatic continental shelf imprinted by oxidation of seeping hydrocarbons. *Mar. Petrol. Geol.*, 66, 511–531.
31. Amano, K., Jenkins, R.G. (2007). Eocene drill holes in cold-seep bivalves of Hokkaido, northern Japan. *Mar. Ecol.*, 28, 108–114.
32. Clari, P., Dela Pierre, F., Martire, L., Cavagna, S. (2009). The Cenozoic CH4-derived carbonates of Monferrato (NW Italy): a solid evidence of fluid circulation in the sedimentary column. *Mar. Geol.*, 265, 167–184.

33. Taylor, J.D., Glover, E.A. (2009). New lucinid bivalves from hydrocarbon seeps of the Western Atlantic (Mollusca: Bivalvia: Lucinidae). *Steenstrupia*, 30, 127–140.

8. Space for notes